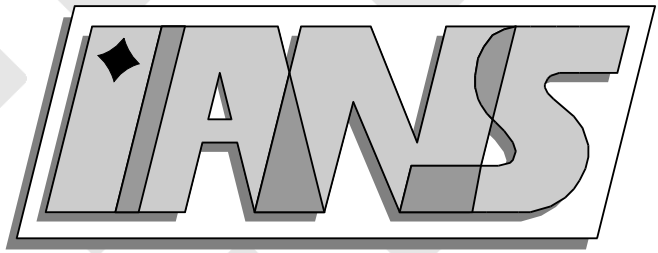


**Universität  
Stuttgart**



---

Local Discontinuous-Galerkin Schemes for Model  
Problems in Phase Transition Theory

Jenny Haink, Christian Rohde

---

**Berichte aus dem Institut für  
Angewandte Analysis und Numerische Simulation**

Preprint 2007/011



---

## Local Discontinuous-Galerkin Schemes for Model Problems in Phase Transition Theory

Jenny Haink, Christian Rohde

---

**Berichte aus dem Institut für  
Angewandte Analysis und Numerische Simulation**

Preprint 2007/011

Institut für Angewandte Analysis und Numerische Simulation (IANS)  
Fakultät Mathematik und Physik  
Fachbereich Mathematik  
Pfaffenwaldring 57  
D-70 569 Stuttgart

**E-Mail:** [ians-preprints@mathematik.uni-stuttgart.de](mailto:ians-preprints@mathematik.uni-stuttgart.de)  
**WWW:** <http://preprints.ians.uni-stuttgart.de>

ISSN **1611-4176**

© Alle Rechte vorbehalten. Nachdruck nur mit Genehmigung des Autors.  
IANS-Logo: Andreas Klimke.  $\LaTeX$ -Style: Winfried Geis, Thomas Merkle.

# Local Discontinuous-Galerkin Schemes for Model Problems in Phase Transition Theory

Jenny Haink and Christian Rohde

ABSTRACT. Local Discontinuous Galerkin (LDG) schemes in the sense of [5] are a flexible numerical tool to approximate solutions of nonlinear convection problems with complicated dissipative terms. Such terms frequently appear in evolution equations which describe the dynamics of phase changes in e.g. liquid-vapour mixtures or in elastic solids. We report on results for one-dimensional model problems with dissipative terms including third-order and convolution operators. Cell entropy inequalities and  $L^2$ -stability results are proved for those model problems. As is common in phase transition theory the solution structure sensitively depends on the coupling parameter between viscosity and capillarity. To avoid spurious solutions due to the counteracting effect of artificial dissipation by the numerical flux and the actual dissipation terms we introduce Tadmors' entropy conservative fluxes. Various numerical experiments underline the reliability of our approach and also illustrate interesting and (partly) new phase transition phenomena.

## 1. Introduction

As a basic model problem we consider the initial value problem

$$(1) \quad u_t^\varepsilon + f(u^\varepsilon)_x = R^\varepsilon[u^\varepsilon] \quad \text{in } D_T := \mathbb{R} \times (0, T), T > 0,$$
$$(2) \quad u^\varepsilon(\cdot, 0) = u_0 \quad \text{in } \mathbb{R}.$$

Here, for  $\varepsilon > 0$ , the unknown function is  $u^\varepsilon : \mathbb{R} \times [0, T] \rightarrow \mathbb{R}$ . By  $f \in C^1(\mathbb{R}, \mathbb{R})$  we denote the given flux function and by  $u_0 \in L^\infty(\mathbb{R}) \cap L^1(\mathbb{R})$  the initial function. Let us assume that (1), (2) is uniquely solvable in an appropriate function space where  $R^\varepsilon$  is a dissipative operator acting on this space. Specific examples are given below.

We are interested in choices of  $R^\varepsilon$  such that

$$(3) \quad \lim_{\varepsilon \rightarrow 0} R^\varepsilon[w] \equiv 0$$

holds for all functions  $w : \mathbb{R} \rightarrow \mathbb{R}$  in the function space at hand in the sense of distributions. Then

(1) turns in the limit  $\varepsilon \rightarrow 0$  into the hyperbolic equation

$$(4) \quad u_t + f(u)_x = 0 \quad \text{in } D_T.$$

Solutions of initial value problems for (4) might contain discontinuous shock waves so that one has to consider weak solutions which, however, are not uniquely determined. In this framework it is natural to enforce uniqueness by selecting the admissible weak solution for (4) as the function  $u : \mathbb{R} \times [0, T] \rightarrow \mathbb{R}$  with

$$(5) \quad \lim_{\varepsilon \rightarrow 0} \|u^\varepsilon - u\|_{L^p_{loc}(D_T)} = 0,$$

---

*Key words and phrases.* Conservation laws, Discontinuous-Galerkin method, Dynamical phase boundaries, Tadmors flux, Convolution operator.

provided the latter limit exists for some  $p \geq 1$  and  $u$  is a weak solution of (4).

For small but positive  $\varepsilon > 0$  in (1) it is a challenge to solve the initial value problem numerically since then the solution is governed by the behaviour of the limit problem and can contain steep internal layers. Additionally the numerical entropy dissipation has to be tuned very carefully since the limit (5) can sensitively depend on the structure of  $R^\varepsilon$  as we shall detail below. The Local Discontinuous Galerkin(LDG)-scheme provides an elegant and flexible tool to treat quite general versions of (1), in particular the (formal) order of the method can be chosen without restrictions. The approach has been originally introduced in [5] for diffusion operators and since then has been applied to many other evolution equations so that we only refer to the overview publications [2, 3]. The LDG-approach relies on a reformulation of (1) as a degenerate first-order system and the discretization of this system by the (classical) Discontinuous-Galerkin method (cf. [4]) for first-order systems. We note also that the LDG-scheme requires to use numerical flux functions to discretize the term  $f(u^\varepsilon)_x$  and the dissipative fluxes that come out of  $R^\varepsilon$  in (1).

In this paper we test the LDG-scheme for complex choices for  $R^\varepsilon$  which have been recently suggested as models for phase transition phenomena. We are interested in cases where the limit in (5) exists but leads to non-standard weak solutions (,i.e., weak solutions which not necessarily are Kruzkov-solutions) of (4).

A well analyzed choice for  $R^\varepsilon$  in (1) such that  $u$  from (5) exists is

$$(6) \quad R^\varepsilon[w] = \varepsilon w_{xx}, \quad w \in C^2(\mathbb{R}).$$

Then for each  $\varepsilon > 0$  an unique classical solution  $u^\varepsilon$  of (1), (2) exists and (a subsequence of)  $\{u^\varepsilon\}_{\varepsilon>0}$  converges for  $\varepsilon \rightarrow 0$  in  $L^1_{loc}(D_T)$  to a function  $u$  which is the Kruzkov-solution of (4).

Intricate solution patterns occur if we choose  $f$  in (1) to be *nonconvex* and consider for  $\lambda \in \mathbb{R}$  the operators

$$(7) \quad R^\varepsilon[w] = \varepsilon w_{xx} + \lambda \varepsilon^2 w_{xxx}, \quad w \in C^3(\mathbb{R})$$

or alternatively

$$(8) \quad R^\varepsilon[w] = \varepsilon w_{xx} + \lambda D^\varepsilon[w]_x, \quad w \in C^2(\mathbb{R}) \cap L^\infty(\mathbb{R}),$$

with the convolution type operator

$$(9) \quad D^\varepsilon[w](x) := \gamma \int_{\mathbb{R}} \Phi_\varepsilon(x-y)(w(y) - w(x)) dy = \gamma([\Phi_\varepsilon * w](x) - w(x))$$

for  $\gamma > 0$ . Throughout the paper we suppose that we have

$$(10) \quad \Phi_\varepsilon(x) = \frac{1}{\varepsilon} \Phi\left(\frac{x}{\varepsilon}\right) \quad \text{for all } x \in \mathbb{R},$$

where  $\Phi$  is an even and, if not stated otherwise, non-negative function from  $C_0^0(\mathbb{R})$  with

$$(11) \quad \int_{\mathbb{R}} \Phi(x) dx = 1.$$

It has been proven that (1), (2) with choices either (7) or (8) has a unique classical solution and that a subsequence of  $\{u^\varepsilon\}_{\varepsilon>0}$  converges to a weak solution of (4). The important point is that the limit function in general does not satisfy all entropy inequalities, thus is not a Kruzkov-solution anymore, and can contain undercompressive shock waves (see [11] for an overview, [18, 9] for the case (7) and [16] for (8)). Moreover the limit sensitively depends on the diffusion-dispersion ratio  $\lambda$ .

Let us make here a remark on the relation between the convolution term  $D^\varepsilon[w]$  and the second-order term  $\varepsilon^2 w_{xx}$ . Provided  $w$  is smooth enough Taylor's expansion theorem gives for  $x \in \mathbb{R}$

$$\begin{aligned} D^\varepsilon[w(\cdot, t)](x) &\approx \gamma \int_{\mathbb{R}} \Phi_\varepsilon(x-y) \left( w_x(x, t)(y-x) + \frac{1}{2} w_{xx}(x, t)(y-x)^2 \right) dy \\ &= \left( \gamma \frac{\varepsilon^2}{2} \int_{\mathbb{R}} \Phi(x) x^2 dx \right) w_{xx}(x, t) \\ &= \varepsilon^2 w_{xx}(x, t), \end{aligned}$$

where we used (11) and defined  $\gamma$  by

$$\gamma = \frac{2}{\int_{\mathbb{R}} \Phi(x)x^2 dx}.$$

With that point of view it makes sense to compare the solutions for local and non-local choices as well as the obtained numerical solutions.

Let us mention that (1), (2) is a simple model problem for the complex Navier-Stokes-Korteweg (NSK)-system. For the local NSK-system, i.e., a right hand side similar to (7), the successful application of the LDG-scheme in two space dimensions as well as theoretical contributions can be found in [6]. For a FD-discretization of (1) with (7) we refer to [1].

In Sect. 2 the LDG-scheme is formulated for (1), (2) with both diffusive-dispersive choices (7) and (8) for  $R^\varepsilon$ . In the non-local case (8) we propose two versions for LDG-discretization, a “flux-” and a “source-like” version. As will be seen in the several numerical examples the source-like scheme produces the clearly better results while the flux-like version is more accessible for analytical treatment. As the main theoretical contribution we present  $L^2$ -stability for the numerical solutions  $u_h$  for both choices (7) and (8). For the LDG-scheme of the local equation (1), (7) a generalized cell entropy inequality is derived (note that for  $R^\varepsilon[w] = w_{xxx}$  this was already done by Yan&Shu in [21]). A non-local counterpart is given for the flux-like LDG-scheme of (1), (8). The discretization of the nonlinear flux term in (1) introduces artificial dissipation which might counteract with the correct dissipation that comes from  $R^\varepsilon$ . To erase this extra term in the cell entropy inequality we suggest to use so-called entropy conservative fluxes proposed by Tadmor [19] (see also [20]) in another context. Note that the idea of entropy conservative fluxes has already been used in [12] to compute diffusive-dispersive limits. Careful numerical experiments with the derived LDG-schemes demonstrate the reliability of the approach and display the complex solution structure of (1), (2) (, e.g. solutions are not necessarily total variation diminishing). By the use of Tadmor’s flux the occurrence of spurious solutions is prohibited (see in particular Testproblem 2 in Sect. 2.3).

As noted before the combination of diffusive and dispersive terms in (7), (8) appears also in and is in fact motivated by more realistic models describing the dynamics of multiphase media (see e.g. [8] for the local problem and [17] for the non-local variant). The terms can be identified with the effects of viscosity and capillarity. A simple but important model to describe phase transition processes is the one-dimensional system of visco-capillar elasticity given by

$$(12) \quad w_t^\varepsilon - v_x^\varepsilon = 0, \quad v_t^\varepsilon - \sigma(w^\varepsilon)_x = \varepsilon v_{xx}^\varepsilon - \lambda \begin{cases} \varepsilon^2 w_{xxx}^\varepsilon \\ D^\varepsilon[w^\varepsilon]_x \end{cases}$$

in  $D_T$  and

$$(13) \quad w^\varepsilon(\cdot, 0) = w_0, \quad v^\varepsilon(\cdot, 0) = v_0 \quad \text{in } \mathbb{R}.$$

Here  $w^\varepsilon : \mathbb{R} \times [0, T) \rightarrow \mathbb{R}$  is the stress and  $v^\varepsilon : \mathbb{R} \times [0, T) \rightarrow \mathbb{R}$  the velocity. The initial velocity  $v_0 : \mathbb{R} \rightarrow \mathbb{R}$  and stress  $w_0 : \mathbb{R} \rightarrow \mathbb{R}$  are given,  $D^\varepsilon$  is as in (9). An exemplary stress-strain relation  $\sigma$  is given by

$$\sigma(w) = w^3 - w,$$

such that  $\sigma$  is non-monotone which allows to define phases: we say that a state  $w$  is in the low (resp. high) strain phase if  $w \in (-\infty, -\sqrt{1/3}]$  (resp.  $w \in [\sqrt{1/3}, \infty)$ ) holds. The graph of  $\sigma$  is displayed in Fig. 1. Note that  $\pm\sqrt{1/3}$  are local extrema of the function.

For classical solutions  $(w^\varepsilon, v^\varepsilon)$  of (12), (13) it is known that the total energy (potential energy + kinetic energy) decays in time (see (43) below). In Sect. 3 a discrete counterpart with a mesh-dependent energy function is proved for the flux-like LDG-scheme of the non-local version in (12). We present computations with the LDG-schemes again relying on entropy conservative flux discretizations and verify that the numerical solutions also satisfy the observed energy decay. Note that it is a remarkable property of the LDG-method using this kind of flux that the energy decreases without spurious oscillations differently from standard discretizations (see e.g. [6]). As examples we show phase coarsening procedures for (7) and (8) with non-negative kernel. We

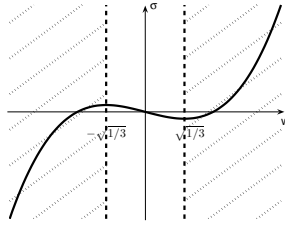


FIGURE 1. Graph of  $\sigma$  and hyperbolic regions of the state space.

remark that for (12), (13) existence results and results on the limit behaviour as  $\varepsilon$  vanishes can be found in [10, 17]. Motivated by the work of Ren&Truskinovsky [15] we finally consider the non-local variant in (12) with a kernel  $\Phi$  that *changes sign*. In contrast to the phase separation problems now multiple phase boundaries persist for large times and can be clearly observed in the numerical experiments. We identify a new one-parameter dependent family of such kernels such that the number of phase boundaries in the large-time regime can be controlled by this parameter. To conclude the introduction let us note that this kind of “microstructure evolution” cannot be modelled with the local approach in (12) up to our knowledge.

## 2. Local and Non-local Diffusive-Dispersive Equations

### 2.1. Formulation of the LDG-Scheme

In this section we consider the initial value problem (1), (2) with  $R^\varepsilon$  given by (7) or (8) and formulate the LDG-scheme following [5]. For the sake of simplicity we omit the dependence on  $\varepsilon$  in this section if not stated otherwise.

We define for  $j \in \mathbb{Z}$  and  $x_{j\pm 1/2} \in \mathbb{R}$  with  $x_{j-1/2} < x_{j+1/2}$  the cells  $I_j := [x_{j-1/2}, x_{j+1/2})$  with local cell size  $h_j := x_{j+1/2} - x_{j-1/2}$ , such that  $\{I_j\}_{j \in \mathbb{Z}}$  is a –not necessarily equidistant– partition of the real line. By  $x_{j+1/2}^\pm$  we denote the left- and right-hand limit to  $x_{j+1/2}$ , i.e.,

$$x_{j+1/2}^- := \lim_{x \nearrow x_{j+1/2}} x, \quad x_{j+1/2}^+ := \lim_{x \searrow x_{j+1/2}} x.$$

Let  $p \in \mathbb{N}$ . For  $t \in [0, T)$  we seek an approximation  $u_h(\cdot, t) : \mathbb{R} \rightarrow \mathbb{R}$  of the solution of (1), (2) in the space

$$\mathcal{V}_h^p := \{ \phi_h \mid \phi_h|_{I_j} \text{ is a polynomial of degree } \leq p-1 \text{ for all } j \in \mathbb{Z} \}.$$

Define for  $k \in \{0, \dots, p-1\}$  the functions

$$\phi_k^j(x) := \begin{cases} p_k^j(x) & : x \in I_j, \\ 0 & : x \in \mathbb{R} \setminus I_j. \end{cases}$$

Here  $p_k^j$  denotes the  $k$ th Legendre polynomial transformed to  $I_j$ . We have  $\mathcal{V}_h^p = \text{span}\{\phi_k^j \mid k = 0, \dots, p-1, j \in \mathbb{Z}\}$ , and thus we make the ansatz

$$(14) \quad u_h(\cdot, t) \Big|_{I_j} = \sum_{k=0}^{p-1} \alpha_k^j(t) \phi_k^j(\cdot),$$

with the unknown coefficients  $\alpha_k^j(t) \in \mathbb{R}$ .

**LDG-Scheme for the Local Diffusive-Dispersive Equation.** Let us consider at first the local version (7). As in [5] we introduce the auxiliary variables  $q := u_x$  and  $p := q_x$  to formally remove the second and third order space-derivatives in (1). That means we rewrite (1) as the



system

$$\begin{aligned} u_t + (f(u) - \varepsilon q - \lambda \varepsilon^2 p)_x &= 0, \\ q - u_x &= 0, \\ p - q_x &= 0. \end{aligned}$$

and seek for solutions  $u_h, q_h, p_h \in \mathcal{V}_h^p$ . For the auxiliary variables we make an ansatz analogue to (14) and obtain

$$(15) \quad q_h(\cdot, t) \Big|_{I_j} = \sum_{k=0}^{p-1} \beta_k^j(t) \phi_k^j(\cdot), \quad p_h(\cdot, t) \Big|_{I_j} = \sum_{k=0}^{p-1} \zeta_k^j(t) \phi_k^j(\cdot).$$

The LDG-scheme now defines the approximations  $u_h(\cdot, t), q_h(\cdot, t), p_h(\cdot, t) : \mathbb{R} \rightarrow \mathbb{R}$  such that they satisfy

$$\begin{aligned} (16) \quad & \int_{I_j} u_{h,t}(x, t) \phi_h(x) dx - \int_{I_j} (f(u_h(x, t)) - \varepsilon q_h(x, t) - \lambda \varepsilon^2 p_h(x, t)) \phi_{h,x}(x) dx \\ &= -\tilde{f}_{j+1/2} \phi_h(x_{j+1/2}^-) + \tilde{f}_{j-1/2} \phi_h(x_{j-1/2}^+) \\ & \quad + \varepsilon \tilde{q}_{j+1/2} \phi_h(x_{j+1/2}^-) - \varepsilon \tilde{q}_{j-1/2} \phi_h(x_{j-1/2}^+) \\ & \quad + \lambda \varepsilon^2 \tilde{p}_{j+1/2} \phi_h(x_{j+1/2}^-) - \lambda \varepsilon^2 \tilde{p}_{j-1/2} \phi_h(x_{j-1/2}^+), \\ & \int_{I_j} q_h(x, t) \phi_h(x) dx + \int_{I_j} u_h(x, t) \phi_{h,x}(x) dx = \tilde{u}_{j+1/2} \phi_h(x_{j+1/2}^-) - \tilde{u}_{j-1/2} \phi_h(x_{j-1/2}^+), \\ & \int_{I_j} p_h(x, t) \phi_h(x) dx + \int_{I_j} q_h(x, t) \phi_{h,x}(x) dx = \tilde{q}_{j+1/2} \phi_h(x_{j+1/2}^-) - \tilde{q}_{j-1/2} \phi_h(x_{j-1/2}^+) \end{aligned}$$

for all  $\phi_h \in \mathcal{V}_h^p$ ,  $j \in \mathbb{Z}$  and  $t \geq 0$ .

By

$$\tilde{f}_{j+1/2} := \tilde{f}(u_h(x_{j+1/2}^-, t), u_h(x_{j+1/2}^+, t))$$

we denote an arbitrary numerical flux function  $\tilde{f} : \mathbb{R}^2 \rightarrow \mathbb{R}$  consistent with  $f$ , i.e.,  $\tilde{f}(w, w) = f(w)$  for all  $w \in \mathbb{R}$ . Later on we use as specific choices E-fluxes as well as Tadmor's flux. For an E-flux

$$(17) \quad \text{sign}(b - a) \left( \tilde{f}(a, b) - f(u) \right) \leq 0 \quad \text{for all } u \in [\min\{a, b\}, \max\{a, b\}]$$

holds true. Tadmor's flux is defined as

$$(18) \quad \tilde{g}(a, b) = \int_0^1 g(a + s(b - a)) ds,$$

where we first rewrite  $g(\xi) = f(u)$  with  $\xi := \eta'(u)$  for some strictly convex function  $\eta : \mathbb{R} \rightarrow \mathbb{R}$  (see [20]). The abbreviations  $\tilde{u}_{j+1/2}, \tilde{q}_{j+1/2}$  and  $\tilde{p}_{j+1/2}$  in (16) stand for central numerical fluxes, i.e.,

$$\begin{aligned} \tilde{u}_{j+1/2} &:= \tilde{u}(u_h(x_{j+1/2}^-, t), u_h(x_{j+1/2}^+, t)), \\ \tilde{q}_{j+1/2} &:= \tilde{q}(q_h(x_{j+1/2}^-, t), q_h(x_{j+1/2}^+, t)), \\ \tilde{p}_{j+1/2} &:= \tilde{p}(p_h(x_{j+1/2}^-, t), p_h(x_{j+1/2}^+, t)) \end{aligned}$$

with  $\tilde{u}, \tilde{q}, \tilde{p} : \mathbb{R}^2 \rightarrow \mathbb{R}$  specified by

$$(19) \quad \tilde{u}/\tilde{q}/\tilde{p}(a, b) = \frac{1}{2}(a + b).$$

Due to the use of Legendre polynomials as basis functions one gets ordinary differential equations resp. explicit formulas for the unknown coefficients in (14), (15), namely

$$\begin{aligned}
(20) \quad \alpha_{k,t}^j &= \frac{2k+1}{h_j} \left\{ \int_{I_j} (f(u_h(x,t)) - \varepsilon q_h(x,t) - \lambda \varepsilon^2 p_h(x,t)) \phi_{k,x}^j(x) dx \right. \\
&\quad - \tilde{f}_{j+1/2} + (-1)^k \tilde{f}_{j-1/2} \\
&\quad + \varepsilon \tilde{q}_{j+1/2} - (-1)^k \varepsilon \tilde{q}_{j-1/2} \\
&\quad \left. + \lambda \varepsilon^2 \tilde{p}_{j+1/2} - (-1)^k \lambda \varepsilon^2 \tilde{p}_{j-1/2} \right\}, \\
\beta_k^j &= \frac{2k+1}{h_j} \left\{ - \int_{I_j} u_h(x,t) \phi_{k,x}^j(x) dx + \tilde{u}_{j+1/2} - (-1)^k \tilde{u}_{j-1/2} \right\}, \\
\zeta_k^j &= \frac{2k+1}{h_j} \left\{ - \int_{I_j} q_h(x,t) \phi_{k,x}^j(x) dx + \tilde{q}_{j+1/2} - (-1)^k \tilde{q}_{j-1/2} \right\}
\end{aligned}$$

for  $k = 0, \dots, p-1$ ,  $j \in \mathbb{Z}$  and  $t \geq 0$ .

Up to now we have not taken into account the initial datum (2). Throughout the paper we initialize the unknown coefficients  $\alpha_k^j(0)$  by the  $L^2$ -projection

$$\alpha_k^j(0) = \frac{2k+1}{h_j} \int_{I_j} u_0(x) \phi_k^j(x) dx$$

to apply the LDG-schemes.

### Flux-like Variant for an LDG-Scheme for the Non-local Diffusive-Dispersive Equation.

In the non-local case (8) there is still the diffusion term  $\varepsilon u_{xx}$  for which we use  $q := u_x$  but there is no need to introduce a second auxiliary variable. Since the convolution integral already emerges in flux form we rewrite (1) as

$$\begin{aligned}
u_t + (f(u) - \varepsilon q - \lambda \gamma (\Phi_\varepsilon * u - u))_x &= 0, \\
q - u_x &= 0.
\end{aligned}$$

Instead of (16) we seek for functions  $u_h, q_h \in \mathcal{V}_h^p$  such that

$$\begin{aligned}
(21) \quad & \int_{I_j} u_{h,t}(x,t) \phi_h(x) dx - \int_{I_j} (f(u_h(x,t)) - \varepsilon q_h(x,t) - \lambda \gamma ([\Phi_\varepsilon * u_h(\cdot, t)](x) - u_h(x,t))) \phi_{h,x}(x) dx \\
&= -\tilde{f}_{j+1/2} \phi_h(x_{j+1/2}^-) + \tilde{f}_{j-1/2} \phi_h(x_{j-1/2}^+) \\
&\quad + \varepsilon \tilde{q}_{j+1/2} \phi_h(x_{j+1/2}^-) - \varepsilon \tilde{q}_{j-1/2} \phi_h(x_{j-1/2}^+) \\
&\quad + \lambda \gamma [\Phi_\varepsilon * u_h(\cdot, t)](x_{j+1/2}) \phi_h(x_{j+1/2}^-) - \lambda \gamma [\Phi_\varepsilon * u_h(\cdot, t)](x_{j-1/2}) \phi_h(x_{j-1/2}^+) \\
&\quad - \lambda \gamma \tilde{u}_{j+1/2} \phi_h(x_{j+1/2}^-) + \lambda \gamma \tilde{u}_{j-1/2} \phi_h(x_{j-1/2}^+), \\
& \int_{I_j} q_h(x,t) \phi_h(x) dx + \int_{I_j} u_h(x,t) \phi_{h,x}(x) dx = \tilde{u}_{j+1/2} \phi_h(x_{j+1/2}^-) - \tilde{u}_{j-1/2} \phi_h(x_{j-1/2}^+)
\end{aligned}$$

holds for all  $\phi_h \in \mathcal{V}_h^p$ ,  $j \in \mathbb{Z}$  and  $t \geq 0$ . By  $\tilde{f}$ ,  $\tilde{u}$  and  $\tilde{q}$  we again denote numerical flux functions. Note that it is not necessary to introduce a numerical flux for the convolution term. Instead we directly evaluate  $[\Phi_\varepsilon * u_h(\cdot, t)](x_{j\pm 1/2})$  at the cell boundaries, because the convolution of  $\Phi_\varepsilon \in C_0^0(\mathbb{R})$  and  $u_h \in L^1(\mathbb{R})$  always yields a continuous result. However, to find the counterpart to (20) we have to look in more detail at the convolution integral

$$\int_{I_j} [\Phi_\varepsilon * u_h(\cdot, t)](x) \phi_{h,x}(x) dx = \int_{I_j} \left( \int_{\mathbb{R}} \Phi_\varepsilon(x-y) u_h(y,t) dy \right) \phi_{h,x}(x) dx.$$

Since the kernel  $\Phi_\varepsilon$  has compact support define  $s(j), S(j) \in \mathbb{N}$  for  $j \in \mathbb{Z}$  such that we have

$$(22) \quad \text{supp}(\Phi_\varepsilon(x - \cdot)) \subset [x_{j-s(j)-1/2}, x_{j+S(j)+1/2}] \quad (x \in I_j, j \in \mathbb{Z}).$$

Note that we skipped the  $\varepsilon$ -dependence for  $s(j), S(j)$ . Since  $u_h$  is a piecewise polynomial in space we split the integration over  $\mathbb{R}$  into several integrals over the cells  $I_j$  and get

$$\int_{I_j} [\Phi_\varepsilon * u_h(\cdot, t)](x) \phi_{h,x}(x) dx = \sum_{i=j-s(j)}^{j+S(j)} \sum_{l=0}^{p-1} \alpha_l^i(t) \int_{I_j} \left( \int_{I_i} \Phi_\varepsilon(x-y) \phi_l^i(y) dy \right) \phi_{h,x}(x) dx.$$

We only have to regard finitely many elements  $I_i$ ,  $i = j-s(j), \dots, j+S(j)$  due to (22). Now with the basis functions  $\phi_k^j$  as test functions we arrive at

$$(23) \quad \begin{aligned} \alpha_{k,t}^j(t) &= \frac{2k+1}{h_j} \left\{ \int_{I_j} (f(u_h(x,t)) - \varepsilon q_h(x,t)) \phi_{k,x}^j(x) dx + \lambda\gamma \sum_{i=j-s(j)}^{j+S(j)} \sum_{l=0}^{p-1} \alpha_l^i(t) \mathcal{J}_{k,l}^{j,i} \right. \\ &\quad \left. - \tilde{f}_{j+1/2} + (-1)^k \tilde{f}_{j-1/2} \right. \\ &\quad \left. + \varepsilon \tilde{q}_{j+1/2} - (-1)^k \varepsilon \tilde{q}_{j-1/2} \right\} - \lambda\gamma \beta_k^j(t), \\ \beta_k^j(t) &= \frac{2k+1}{h_j} \left\{ - \int_{I_j} u_h(x,t) \phi_{k,x}^j(x) dx + \tilde{u}_{j+1/2} - (-1)^k \tilde{u}_{j-1/2} \right\} \end{aligned}$$

for  $k = 0, \dots, p-1$ ,  $j \in \mathbb{Z}$  and  $t \geq 0$ . We used

$$(24) \quad \begin{aligned} \mathcal{J}_{k,l}^{j,i} &:= - \int_{I_j} \left( \int_{I_i} \Phi_\varepsilon(x-y) \phi_l^i(y) dy \right) \phi_{k,x}^j(x) dx \\ &\quad + \int_{I_i} \Phi_\varepsilon(x_{j+1/2} - y) \phi_l^i(y) dy - (-1)^k \int_{I_i} \Phi_\varepsilon(x_{j-1/2} - y) \phi_l^i(y) dy \end{aligned}$$

for  $k, l = 0, \dots, p-1$ ,  $j \in \mathbb{Z}$ ,  $i = j-s(j), \dots, j+S(j)$ , where the last two integrals are related to the cell boundary terms  $[\Phi_\varepsilon * u_h(\cdot, t)](x_{j\pm 1/2}) \phi_h(x_{j\pm 1/2})$  in (21).

Now if we compare both schemes, (20) and (23), the advantage in the non-local version is that (on a fixed grid) the values  $\mathcal{J}_{k,l}^{j,i}$  do not change during computing time in contrast to the unknown coefficients  $\zeta_k^j$  in (20). For that reason we have to calculate them only once.

**Source-like Variant for an LDG-Scheme for the Non-local Diffusive-Dispersive Equation.** Another possibility to treat the convolution term in (8) is to first rewrite  $D^\varepsilon[w]_x = D^\varepsilon[q]$  with an auxiliary variable  $q = w_x$ . Then for the system

$$\begin{aligned} u_t + (f(u) - \varepsilon q)_x - \lambda\gamma(\Phi_\varepsilon * q - q) &= 0, \\ q - u_x &= 0. \end{aligned}$$

we perform an analogue LDG-discretization as in the case of the flux-like treated convolution term, i.e., we have

$$(25) \quad \begin{aligned} &\int_{I_j} (u_{h,t}(x,t) - \lambda\gamma([\Phi_\varepsilon * q_h(\cdot, t)](x) - q_h(x,t))) \phi_h(x) dx - \int_{I_j} (f(u_h(x,t)) - \varepsilon q_h(x,t)) \phi_{h,x}(x) dx \\ &= -\tilde{f}_{j+1/2} \phi_h(x_{j+1/2}^-) + \tilde{f}_{j-1/2} \phi_h(x_{j-1/2}^+) \\ &\quad + \varepsilon \tilde{q}_{j+1/2} \phi_h(x_{j+1/2}^-) - \varepsilon \tilde{q}_{j-1/2} \phi_h(x_{j-1/2}^+), \\ &\int_{I_j} q_h(x,t) \phi_h(x) dx + \int_{I_j} u_h(x,t) \phi_{h,x}(x) dx = \tilde{u}_{j+1/2} \phi_h(x_{j+1/2}^-) - \tilde{u}_{j-1/2} \phi_h(x_{j-1/2}^+) \end{aligned}$$

for all  $\phi_h \in \mathcal{V}_h^p$ ,  $j \in \mathbb{Z}$  and  $t \geq 0$ . Here for the test functions  $\phi_h = \phi_k^j$ ,  $k = 0, \dots, p-1$ ,  $j \in \mathbb{Z}$ , we obtain

$$\int_{I_j} [\Phi_\varepsilon * q_h(\cdot, t)](x) \phi_k^j(x) dx = \sum_{i=j-s(j)}^{j+S(j)} \sum_{l=0}^{p-1} \beta_l^i(t) \bar{\mathcal{J}}_{k,l}^{j,i}$$

for

$$(26) \quad \bar{\mathcal{J}}_{k,l}^{j,i} := \int_{I_j} \left( \int_{I_i} \Phi_\varepsilon(x-y) \phi_l^i(y) dy \right) \phi_k^j(x) dx$$

and  $k, l = 0, \dots, p-1$ ,  $j \in \mathbb{Z}$ ,  $i = j-s(j), \dots, j+S(j)$ . Note that there are no cell boundary terms  $[\Phi_\varepsilon * u_h(\cdot, t)](x_{j\pm 1/2}) \phi_h(x_{j\pm 1/2}^\mp)$  as in the flux-like version of the non-local LDG-scheme (21).

At the end of this section we will compare the numerical solutions for both of these non-local variants of the LDG-scheme. By  $u_{h,global_f}$  (resp.  $u_{h,global_s}$ ) we denote the solution  $u_h \in \mathcal{V}_h^p$  that comes out of (21) (resp. (25)). To evaluate the remaining integrals in (20), (23) – (26) we use sufficiently high order quadrature rules. Time discretization for the ordinary differential equations in (20), (23) and obtained by (25) is done by appropriate Runge-Kutta schemes.

## 2.2. Generalized Cell Entropy Inequality and $L^2$ -Stability

**Local Diffusive-Dispersive Equation.** Before we turn to numerics we note that for any smooth solution  $u$  of (1), (7) which decays sufficiently fast together with its spatial derivatives as  $x \rightarrow \pm\infty$  we have

$$(27) \quad \frac{d}{dt} \int_{\mathbb{R}} \frac{u^2(x, t)}{2} dx + \varepsilon \int_{\mathbb{R}} u_x^2(x, t) dx = 0 \quad \text{for all } t \geq 0.$$

In general one can not expect that all  $L^p$ -norms for  $p \in [1, \infty) \cup \{\infty\}$  are dissipated in contrast to the parabolic regularization  $R^\varepsilon[w] = \varepsilon w_{xx}$  in (1), as will be pointed out by the numerical experiments at the end of this section (see also [9]).

We have the following cell entropy inequality for the semidiscrete scheme (16).

**Theorem 2.1** (Generalized Cell Entropy Inequality). *Let  $u_h \in \mathcal{V}_h^p$  be the solution of the LDG-scheme (16), where  $\tilde{u}, \tilde{q}, \tilde{p}$  are central fluxes as in (19).*

(i) *Let  $\tilde{f}$  be an E-flux, i.e., (17) holds true. Then there exist functions*

$$\theta_{j-1/2} = \theta(u_h(x_{j-1/2}^-, t), u_h(x_{j-1/2}^+, t))$$

with  $\theta_{j-1/2} \geq 0$  for all  $j \in \mathbb{Z}$ ,  $t \geq 0$ , and

$$g_{j+1/2} = g(u_h(x_{j+1/2}^-, t), u_h(x_{j+1/2}^+, t), q_h(x_{j+1/2}^-, t), q_h(x_{j+1/2}^+, t), p_h(x_{j+1/2}^-, t), p_h(x_{j+1/2}^+, t))$$

with  $g(w, w, 0, 0, 0, 0) = f(w)w - F(w)$ , for  $w \in \mathbb{R}$  and a primitive  $F$  of  $f$ , such that  $u_h$  satisfies the generalized cell entropy inequality

$$(28) \quad \frac{d}{dt} \int_{I_j} \frac{u_h^2(x, t)}{2} dx + g_{j+1/2} - g_{j-1/2} = -\varepsilon \int_{I_j} q_h^2(x, t) dx - \theta_{j-1/2} \leq 0$$

for all  $j \in \mathbb{Z}$ ,  $t \geq 0$ .

(ii) *Let  $\tilde{f}$  be Tadmor's flux (18). Then (28) holds with  $\theta_{j-1/2} = 0$  for all  $j \in \mathbb{Z}$ ,  $t \geq 0$ .*

*Proof.* (i) For the test functions  $\phi_h \in \mathcal{V}_h^p$  and  $t \geq 0$  fixed we use  $\phi_h = u_h(\cdot, t)$  in the first,  $\phi_h = \varepsilon q_h(\cdot, t) + \lambda \varepsilon^2 p_h(\cdot, t)$  in the second as well as  $\phi_h = -\lambda \varepsilon^2 q_h(\cdot, t)$  in the third equation of (16)

and sum up all three equations. Then we get

$$\begin{aligned}
0 &= \int_{I_j} u_{h,t}(x,t)u_h(x,t) dx - \int_{I_j} f(u_h(x,t))u_{h,x}(x,t) dx + \varepsilon \int_{I_j} q_h^2(x,t) dx \\
&+ \varepsilon \int_{I_j} (q_h(x,t)u_{h,x}(x,t) + u_h(x,t)q_{h,x}(x,t)) dx \\
&+ \lambda\varepsilon^2 \int_{I_j} (p_h(x,t)u_{h,x}(x,t) + u_h(x,t)p_{h,x}(x,t)) dx - \lambda\varepsilon^2 \int_{I_j} q_h(x,t)q_{h,x}(x,t) dx \\
&+ \tilde{f}_{j+1/2}u_h(x_{j+1/2}^-,t) - \tilde{f}_{j-1/2}u_h(x_{j-1/2}^+,t) \\
&- \varepsilon (\tilde{u}_{j+1/2}q_h(x_{j+1/2}^-,t) + \tilde{q}_{j+1/2}u_h(x_{j+1/2}^-,t)) \\
&+ \varepsilon (\tilde{u}_{j-1/2}q_h(x_{j-1/2}^+,t) + \tilde{q}_{j-1/2}u_h(x_{j-1/2}^+,t)) \\
&- \lambda\varepsilon^2 (\tilde{u}_{j+1/2}p_h(x_{j+1/2}^-,t) + \tilde{p}_{j+1/2}u_h(x_{j+1/2}^-,t)) \\
&+ \lambda\varepsilon^2 (\tilde{u}_{j-1/2}p_h(x_{j-1/2}^+,t) + \tilde{p}_{j-1/2}u_h(x_{j-1/2}^+,t)) \\
&+ \lambda\varepsilon^2 \tilde{q}_{j+1/2}q_h(x_{j+1/2}^-,t) - \lambda\varepsilon^2 \tilde{q}_{j-1/2}q_h(x_{j-1/2}^+,t) \\
&= \frac{d}{dt} \int_{I_j} \frac{u_h^2(x,t)}{2} dx + \varepsilon \int_{I_j} q_h^2(x,t) dx - F(u_h(x_{j+1/2}^-,t)) + F(u_h(x_{j-1/2}^+,t)) \\
&+ \tilde{f}_{j+1/2}u_h(x_{j+1/2}^-,t) - \tilde{f}_{j-1/2}u_h(x_{j-1/2}^+,t) \\
&+ \varepsilon (u_h(x_{j+1/2}^-,t)q_h(x_{j+1/2}^-,t) - \tilde{u}_{j+1/2}q_h(x_{j+1/2}^-,t) - \tilde{q}_{j+1/2}u_h(x_{j+1/2}^-,t)) \\
&- \varepsilon (u_h(x_{j-1/2}^+,t)q_h(x_{j-1/2}^+,t) - \tilde{u}_{j-1/2}q_h(x_{j-1/2}^+,t) - \tilde{q}_{j-1/2}u_h(x_{j-1/2}^+,t)) \\
&+ \lambda\varepsilon^2 (u_h(x_{j+1/2}^-,t)p_h(x_{j+1/2}^-,t) - \tilde{u}_{j+1/2}p_h(x_{j+1/2}^-,t) - \tilde{p}_{j+1/2}u_h(x_{j+1/2}^-,t)) \\
&- \lambda\varepsilon^2 (u_h(x_{j-1/2}^+,t)p_h(x_{j-1/2}^+,t) - \tilde{u}_{j-1/2}p_h(x_{j-1/2}^+,t) - \tilde{p}_{j-1/2}u_h(x_{j-1/2}^+,t)) \\
&- \lambda\varepsilon^2 \left( \frac{1}{2}q_h^2(x_{j+1/2}^-,t) - \tilde{q}_{j+1/2}q_h(x_{j+1/2}^-,t) \right) \\
&+ \lambda\varepsilon^2 \left( \frac{1}{2}q_h^2(x_{j-1/2}^+,t) - \tilde{q}_{j-1/2}q_h(x_{j-1/2}^+,t) \right).
\end{aligned}$$

That is (28) for

$$\begin{aligned}
g_{j+1/2} &= g(u_h(x_{j+1/2}^-,t), u_h(x_{j+1/2}^+,t), q_h(x_{j+1/2}^-,t), q_h(x_{j+1/2}^+,t), p_h(x_{j+1/2}^-,t), p_h(x_{j+1/2}^+,t)) \\
&:= -F(u_h(x_{j+1/2}^-,t)) + \tilde{f}(u_h(x_{j+1/2}^-,t), u_h(x_{j+1/2}^+,t))u_h(x_{j+1/2}^-,t) \\
&+ \varepsilon (u_h(x_{j+1/2}^-,t)q_h(x_{j+1/2}^-,t) - \tilde{u}(u_h(x_{j+1/2}^-,t), u_h(x_{j+1/2}^+,t))q_h(x_{j+1/2}^-,t) \\
&\quad - \tilde{q}(q_h(x_{j+1/2}^-,t), q_h(x_{j+1/2}^+,t))u_h(x_{j+1/2}^-,t)) \\
&+ \lambda\varepsilon^2 (u_h(x_{j+1/2}^-,t)p_h(x_{j+1/2}^-,t) - \tilde{u}(u_h(x_{j+1/2}^-,t), u_h(x_{j+1/2}^+,t))p_h(x_{j+1/2}^-,t) \\
&\quad - \tilde{p}(p_h(x_{j+1/2}^-,t), p_h(x_{j+1/2}^+,t))u_h(x_{j+1/2}^-,t)) \\
&- \lambda\varepsilon^2 \left( \frac{1}{2}q_h^2(x_{j+1/2}^-,t) - \tilde{q}(q_h(x_{j+1/2}^-,t), q_h(x_{j+1/2}^+,t))q_h(x_{j+1/2}^-,t) \right),
\end{aligned}$$

where  $F$  is a primitive of the flux  $f$ , and

$$(29) \quad \begin{aligned} \theta_{j-1/2} &= \theta(u_h(x_{j-1/2}^-, t), u_h(x_{j-1/2}^+, t)) \\ &:= \int_{u_h(x_{j-1/2}^-, t)}^{u_h(x_{j-1/2}^+, t)} \left( f(u) - \tilde{f}(u_h(x_{j-1/2}^-, t), u_h(x_{j-1/2}^+, t)) \right) du, \end{aligned}$$

thanks to the central fluxes  $\tilde{u}, \tilde{q}$  and  $\tilde{p}$ . Finally with the use of (17) we have  $\theta_{j-1/2} \geq 0$  for all  $j \in \mathbb{Z}$ ,  $t \geq 0$ .

(ii) For  $\eta(u) = \frac{u^2}{2}$  in the definition of Tadmor's flux (see (18)) we obtain  $g \equiv f$ , i.e.,

$$\tilde{f}(a, b) = \int_0^1 f(a + s(b-a)) ds = \frac{1}{b-a} \int_a^b f(u) du$$

and thus  $\theta_{j-1/2} = 0$  for all  $j \in \mathbb{Z}$ ,  $t \geq 0$  (see (29)).  $\square$

Let the numerical solutions satisfy

$$(30) \quad |u_h(x, t)|, |q_h(x, t)|, |p_h(x, t)| \rightarrow 0 \quad \text{for } x \rightarrow \pm\infty, t \geq 0.$$

Then after adding up the above cell entropy inequality over all intervals  $\{I_j\}_{j \in \mathbb{Z}}$  we finally observe the

**Corollary 2.2** ( $L^2$ -Stability for (16)). *Let  $u_0 \in L^2(\mathbb{R})$  and  $\tilde{f}$  be continuous. Then with the assumptions of Theorem 2.1 and the property (30) the solution  $u_h \in \mathcal{V}_h^p$  of (16) satisfies*

$$\frac{d}{dt} \int_{\mathbb{R}} \frac{u_h^2(x, t)}{2} dx \leq 0$$

for all  $t \geq 0$ .

**Non-local Diffusive-Dispersive Equation.** For smooth solutions of the non-local diffusive-dispersive problem (1), (8) we also have a decreasing  $L^2$ -norm, i.e., (27) holds true, if  $u$  and  $u_x$  decay sufficiently fast as  $x \rightarrow \pm\infty$ . This is clear if we multiply (1), (8) by  $u$ , integrate over  $\mathbb{R}$  and observe that for some smooth function  $w : \mathbb{R} \rightarrow \mathbb{R}$

$$\begin{aligned} \int_{\mathbb{R}} [\Phi_\varepsilon * w]_x(x) w(x) dx &= \int_{\mathbb{R}} \left( \int_{\mathbb{R}} \Phi_\varepsilon(x-y) w(y) dy \right)_x w(x) dx \\ &= \int_{\mathbb{R}} \left( \int_{\mathbb{R}} \Phi_\varepsilon(z) w_x(x-z) dz \right) w(x) dx \\ &= \int_{\mathbb{R}} \int_{\mathbb{R}} \Phi_\varepsilon(x-y) w_y(y) w(x) dy dx \\ &= \int_{\mathbb{R}} [\Phi_\varepsilon * w](y) w_y(y) dy \\ &= - \int_{\mathbb{R}} [\Phi_\varepsilon * w]_y(y) w(y) dy \end{aligned}$$

holds true. As in the local case it can not be expected that all  $L^p$ -norms for  $p \in [1, \infty) \cup \{\infty\}$  decrease in time.

Differently from (16) there is no cell entropy inequality like in Theorem 2.1 for the non-local counterpart (21) or (25). But we prove the following theorem and finally  $L^2$ -stability for the numerical solution  $u_h$  of (21).

**Theorem 2.3.** *Let  $u_h \in \mathcal{V}_h^p$  be the solution of the LDG-scheme (21), where  $\tilde{u}, \tilde{q}$  are central fluxes as in (19) and  $\tilde{f}$  is an arbitrary numerical flux function. Then there exist functions*

$$\theta_{j-1/2} = \theta(u_h(x_{j-1/2}^-, t), u_h(x_{j-1/2}^+, t))$$

and

$$g_{j+1/2} = g(u_h(x_{j+1/2}^-, t), u_h(x_{j+1/2}^+, t), q_h(x_{j+1/2}^-, t), q_h(x_{j+1/2}^+, t))$$

with  $g(w, w, 0, 0) = f(w)w - F(w)$ , for  $w \in \mathbb{R}$  and a primitive  $F$  of  $f$  such that  $u_h$  satisfies

$$(31) \quad \begin{aligned} & \frac{d}{dt} \int_{I_j} \frac{u_h^2(x, t)}{2} dx + g_{j+1/2} - g_{j-1/2} = -\varepsilon \int_{I_j} q_h^2(x, t) dx - \theta_{j-1/2} \\ & - \lambda\gamma \left( \int_{I_j} [\Phi_\varepsilon * u_h(\cdot, t)](x) u_{h,x}(x, t) dx + [\Phi_\varepsilon * u_h(\cdot, t)](x_{j-1/2}) \left( u_h(x_{j-1/2}^+, t) - u_h(x_{j-1/2}^-, t) \right) \right) \\ & + \lambda\gamma \left( \int_{I_j} u_h(x, t) u_{h,x}(x, t) dx + \tilde{u}_{j-1/2} \left( u_h(x_{j-1/2}^+, t) - u_h(x_{j-1/2}^-, t) \right) \right) \end{aligned}$$

for all  $j \in \mathbb{Z}$ ,  $t \geq 0$ .

*Proof.* For  $t \geq 0$  we choose the test functions  $\phi_h = u_h(\cdot, t)$  in the first and  $\phi_h = \varepsilon q_h(\cdot, t)$  in the second equation of (21) and sum up both equations to get

$$\begin{aligned} 0 &= \frac{d}{dt} \int_{I_j} \frac{u_h^2(x, t)}{2} dx + \varepsilon \int_{I_j} q_h^2(x, t) dx + \lambda\gamma \int_{I_j} ([\Phi_\varepsilon * u_h(\cdot, t)](x) - u_h(x, t)) u_{h,x}(x, t) dx \\ & - F(u_h(x_{j+1/2}^-, t)) + F(u_h(x_{j-1/2}^+, t)) + \tilde{f}_{j+1/2} u_h(x_{j+1/2}^-, t) - \tilde{f}_{j-1/2} u_h(x_{j-1/2}^+, t) \\ & + \varepsilon \left( u_h(x_{j+1/2}^-, t) q_h(x_{j+1/2}^-, t) - \tilde{u}_{j+1/2} q_h(x_{j+1/2}^-, t) - \tilde{q}_{j+1/2} u_h(x_{j+1/2}^-, t) \right) \\ & - \varepsilon \left( u_h(x_{j-1/2}^+, t) q_h(x_{j-1/2}^+, t) - \tilde{u}_{j-1/2} q_h(x_{j-1/2}^+, t) - \tilde{q}_{j-1/2} u_h(x_{j-1/2}^+, t) \right) \\ & - \lambda\gamma \left( [\Phi_\varepsilon * u_h(\cdot, t)](x_{j+1/2}) - \tilde{u}_{j+1/2} \right) u_h(x_{j+1/2}^-, t) \\ & + \lambda\gamma \left( [\Phi_\varepsilon * u_h(\cdot, t)](x_{j-1/2}) - \tilde{u}_{j-1/2} \right) u_h(x_{j-1/2}^+, t). \end{aligned}$$

Now we obtain (31) if we define

$$\begin{aligned} g_{j+1/2} &= g(u_h(x_{j+1/2}^-, t), u_h(x_{j+1/2}^+, t), q_h(x_{j+1/2}^-, t), q_h(x_{j+1/2}^+, t)) \\ & := -F(u_h(x_{j+1/2}^-, t)) + \tilde{f}(u_h(x_{j+1/2}^-, t), u_h(x_{j+1/2}^+, t)) u_h(x_{j+1/2}^-, t) \\ & + \varepsilon \left( u_h(x_{j+1/2}^-, t) q_h(x_{j+1/2}^-, t) - \tilde{u}(u_h(x_{j+1/2}^-, t), u_h(x_{j+1/2}^+, t)) q_h(x_{j+1/2}^-, t) \right. \\ & \quad \left. - \tilde{q}(q_h(x_{j+1/2}^-, t), q_h(x_{j+1/2}^+, t)) u_h(x_{j+1/2}^-, t) \right) \\ & - \lambda\gamma \left( [\Phi_\varepsilon * u_h(\cdot, t)](x_{j+1/2}) - \tilde{u}(u_h(x_{j+1/2}^-, t), u_h(x_{j+1/2}^+, t)) \right) u_h(x_{j+1/2}^-, t) \end{aligned}$$

with a primitive  $F$  of the flux  $f$ , and  $\theta_{j-1/2}$  as in (29). Note that we made use of the central form (19) of the fluxes  $\tilde{u}, \tilde{q}$ .  $\square$

**Corollary 2.4** ( $L^2$ -Stability for (21)). *Let  $u_0 \in L^2(\mathbb{R})$  and  $\tilde{f}$  be a continuous E-flux or Tadmor's flux. Then with the assumptions of Theorem 2.3 and the property (30) for  $u_h, q_h \in \mathcal{V}_h^p$  the solution of (21) satisfies*

$$\frac{d}{dt} \int_{\mathbb{R}} \frac{u_h^2(x, t)}{2} dx \leq 0$$

for all  $t \geq 0$ .

*Proof.* With the definition (17) of an E-flux (resp. (18) of Tadmor's flux) we observe  $\theta_{j-1/2} \geq 0$  (resp.  $\theta_{j-1/2} = 0$ ) for all  $j \in \mathbb{Z}$ ,  $t \geq 0$  (see (29)). Now  $L^2$ -stability follows from (31) after summing up over all intervals  $\{I_j\}_{j \in \mathbb{Z}}$  if we verify that the last two terms in (31) vanish. This is true because

with (30) we have

$$\begin{aligned}
& \sum_{j \in \mathbb{Z}} \left( \int_{I_j} u_h(x, t) u_{h,x}(x, t) dx + \tilde{u}_{j-1/2} \left( u_h(x_{j-1/2}^+, t) - u_h(x_{j-1/2}^-, t) \right) \right) \\
&= \sum_{j \in \mathbb{Z}} \left( \int_{I_j} \left( \frac{u_h^2(x, t)}{2} \right)_x dx + \frac{1}{2} \left( u_h^2(x_{j-1/2}^+, t) - u_h^2(x_{j-1/2}^-, t) \right) \right) \\
&= \frac{1}{2} \sum_{j \in \mathbb{Z}} \left( u_h^2(x_{j+1/2}^-, t) - u_h^2(x_{j-1/2}^-, t) \right) \\
&= 0
\end{aligned}$$

and furthermore

$$\begin{aligned}
& \sum_{j \in \mathbb{Z}} \left( \int_{I_j} [\Phi_\varepsilon * u_h(\cdot, t)](x) u_{h,x}(x, t) dx + [\Phi_\varepsilon * u_h(\cdot, t)](x_{j-1/2}) \left( u_h(x_{j-1/2}^+, t) - u_h(x_{j-1/2}^-, t) \right) \right) \\
&= - \sum_{j \in \mathbb{Z}} \left( \int_{I_j} [\Phi_\varepsilon * u_h(\cdot, t)]_x(x) u_h(x, t) dx \right. \\
&\quad \left. + [\Phi_\varepsilon * u_h(\cdot, t)](x_{j+1/2}) u_h(x_{j+1/2}^-, t) - [\Phi_\varepsilon * u_h(\cdot, t)](x_{j-1/2}) u_h(x_{j-1/2}^-, t) \right) \\
&= - \sum_{j \in \mathbb{Z}} \int_{I_j} \left[ \sum_{k \in \mathbb{Z}} \int_{I_k} \Phi_\varepsilon(x-y) u_h(y, t) dy \right]_x u_h(x, t) dx \\
&= - \sum_{j \in \mathbb{Z}} \int_{I_j} \left[ \sum_{k \in \mathbb{Z}} - \int_{x-x_{k-1/2}}^{x-x_{k+1/2}} \Phi_\varepsilon(z) u_h(x-z, t) dz \right]_x u_h(x, t) dx \\
&= - \sum_{j \in \mathbb{Z}} \sum_{k \in \mathbb{Z}} \int_{I_j} \left( \int_{I_k} \Phi_\varepsilon(x-y) u_{h,y}(y, t) dy \right. \\
&\quad \left. - \Phi_\varepsilon(x-x_{k+1/2}) u_h(x_{k+1/2}^-, t) + \Phi_\varepsilon(x-x_{k-1/2}) u_h(x_{k-1/2}^+, t) \right) u_h(x, t) dx \\
&= - \sum_{k \in \mathbb{Z}} \left( \int_{I_k} \left[ \sum_{j \in \mathbb{Z}} \int_{I_j} \Phi_\varepsilon(y-x) u_h(x, t) dx \right] u_{h,y}(y, t) dy \right. \\
&\quad \left. - [\Phi_\varepsilon * u_h(\cdot, t)](x_{k+1/2}) u_h(x_{k+1/2}^-, t) + [\Phi_\varepsilon * u_h(\cdot, t)](x_{k-1/2}) u_h(x_{k-1/2}^+, t) \right) \\
&= - \sum_{k \in \mathbb{Z}} \left( \int_{I_k} [\Phi_\varepsilon * u_h(\cdot, t)](y) u_{h,y}(y, t) dy \right. \\
&\quad \left. + [\Phi_\varepsilon * u_h(\cdot, t)](x_{k-1/2}) \left( u_h(x_{k-1/2}^+, t) - u_h(x_{k-1/2}^-, t) \right) \right).
\end{aligned}$$

Note that we have used the symmetry of the kernel function  $\Phi_\varepsilon$ . □

### 2.3. Numerical Experiments

Before we start with computations for the diffusive-dispersive equations (1) let us consider (4) for the nonconvex flux function  $f(u) = u^3$  together with the initial datum

$$(32) \quad u_0(x) = \begin{cases} u_l = 1.2 & : x \leq 0.1, \\ u_r = -0.65 & : x > 0.1. \end{cases}$$



Then the function

$$(33) \quad u^0(x) = \begin{cases} u_l & : x \leq 0.1 + s_1 t, \\ u_m & : 0.1 + s_1 t < x \leq 0.1 + s_2 t, \\ u_r & : x > 0.1 + s_2 t \end{cases}$$

for the constant middle state  $u_m = -u_l + \frac{1}{3}\sqrt{\frac{2}{\lambda}} \approx -0.964$  and the shock speeds  $s_1 = \frac{u_l^3 - u_m^3}{u_l - u_m} \approx 1.213$ ,  $s_2 = \frac{u_r^3 - u_m^3}{u_r - u_m} \approx 1.979$  is a weak solution of (4). Note that the slower shock is a so called nonclassical (undercompressive) shock while the faster one is a Lax shock (see e.g. [11]).

**Testproblem 1a.** To test the LDG-schemes we consider the regularized problem (1) in  $[0, 1] \times (0, T)$  with the right hand side (7) resp. (8), the flux  $f(u) = u^3$  and the initial datum (32). The parameters are set to  $\varepsilon = 0.004$  and  $\lambda = 4$ . Then in the local case (7)  $u^0$  in (33) is the limit solution for vanishing  $\varepsilon$ , i.e.,  $u^0 = \lim_{\varepsilon \searrow 0} u^\varepsilon$  (see [18]). Although (33) is not the exact solution of the regularized problem (1) we expect that e.g. the middle state for small  $\varepsilon > 0$  should be close to  $u_m$ . For the non-local problem (1), (8) [16] and numerical experiments suggest that (33) is the correct vanishing- $\varepsilon$ -solution, too.

In the following examples we use the local Lax-Friedrichs flux

$$\tilde{f}(a, b) = \frac{1}{2}(f(a) + f(b) - C(b - a)), \quad \text{with } C = \max_{\min\{a, b\} \leq u \leq \max\{a, b\}} |f'(u)|$$

for  $\tilde{f}_{j+1/2} = \tilde{f}(u_h(x_{j+1/2}^-, t), u_h(x_{j+1/2}^+, t))$  and in the non-local LDG-schemes (21), (25) the kernel function

$$\Phi(x) = \begin{cases} \frac{\exp(1/(x^2-1))}{\int_{-1}^1 \exp(1/(y^2-1)) dy} & : x \in (-1, 1), \\ 0 & : \text{otherwise,} \end{cases}$$

whereas  $\Phi_\varepsilon$  is given as in (10). Fig. 2 shows the numerical results on an equidistant partition  $\{I_j\}_{j=1, \dots, N}$  of  $[0, 1]$  consisting of  $N = 200$  cells. We compare the respective solutions  $u_h \in \mathcal{V}_h^p$  for  $p = 1, 2, 3$  (piecewise constant, linear, quadratic), on the one hand for the local LDG-scheme (16) (see Fig. 2, upper row), on the other hand for the non-local flux- resp. source-like variants of the LDG-scheme as in (21) resp. (25) (see Fig. 2, middle resp. lower row). The thin lines in Fig. 2 show the positions of the shocks as well as the middle state of (33).

In all three variants of the LDG-scheme a distinct improvement is recognizable for greater  $p$ . Hence it really makes sense to increase the order of the LDG-scheme. However comparing all three piecewise constant approximations (see Fig. 2, (a), (d), (g)) the non-local solution  $u_{h, global_s}$  that comes out of the source-like scheme (25) is already closer to the limit solution (33) even on the coarser grid. Only after refining the grid the shape of the piecewise constant solutions (a) and (d) in Fig. 2 tends towards the shocks with speed  $s_1, s_2$  and the correct middle state  $u_m$  (see Fig. 3 for the local case). Indeed the flux-like non-local LDG-scheme (21) gives the worst results in this experiment (see Fig. 2, middle row) and the discretization (25) for the rewritten convolution term  $D^\varepsilon[w]_x = D^\varepsilon[q]$  seems to be the better alternative.

**Testproblem 1b.** The convergence to the limit solution  $u^0$  in (33) is underlined by Table 4 where we display the error  $\|u_{h, local}^\varepsilon - u^0\|_{L^1}$  for various  $\varepsilon$ . Here  $u_{h, local}^\varepsilon \in \mathcal{V}_h^p$  is the solution of the local LDG-scheme (16). We use  $p = 2$  and  $p = 3$ . The corresponding graphs for  $u_{h, local}^\varepsilon$  can be found in Fig. 5. Note that the grid consisting of  $N = 200$  cells is not fine enough to resolve the piecewise linear solution  $u_{h, local}^\varepsilon$  for  $\varepsilon = 0.001$ , especially near the shocks, whereas the piecewise quadratic solution further tends to the correct shock-shock-result (33).

**Testproblem 1c.** Note that we didn't use any slope-limiter in the LDG-schemes. Diffusive-dispersive regularizations like (7), (8) are examples where the use of slope-limiters is counterproductive. Indeed we could use them but then a finer grid is needed in order to make the numerical solution tending towards the limit solution (33) (see Fig. 6 for the example  $u_{h, local} \in \mathcal{V}_h^2$ ).

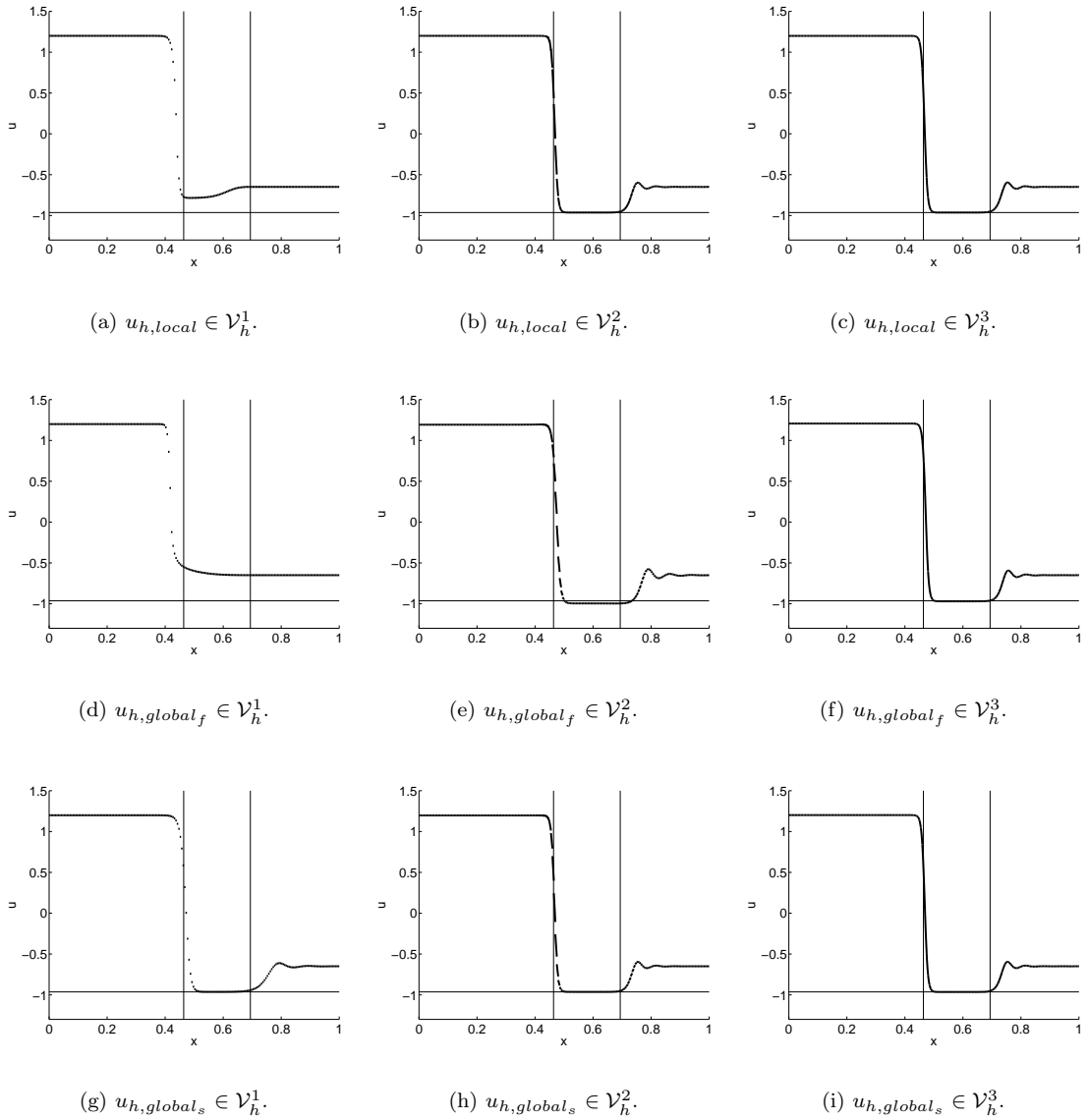


FIGURE 2. Numerical solutions of (1) with (7) (upper row) or (8) (middle and lower row) on an equidistant partition  $\{I_j\}_{j=1,\dots,N}$  ( $N = 200$ ) of  $[0, 1]$  at the time  $t = 0.3$ .

The limit solution  $u^0$  consists of an undercompressive shock and a Lax shock. The thin lines indicate the positions of these shock waves and the middle state at  $t = 0.3$ .

**Testproblem 2.** Not only with the slope-limiter but also with the numerical flux function one has to be careful as will be seen in the next experiment. Until now we used the local Lax-Friedrichs flux. Here we moreover consider the Upwind flux  $\tilde{f}_{j+1/2} = f(u_h(x_{j+1/2}^-, t)) = u_h^3(x_{j+1/2}^-, t)$  and Tadmor's flux (18), which is given by

$$\tilde{f}(a, b) = \frac{1}{4}(a + b)(a^2 + b^2)$$

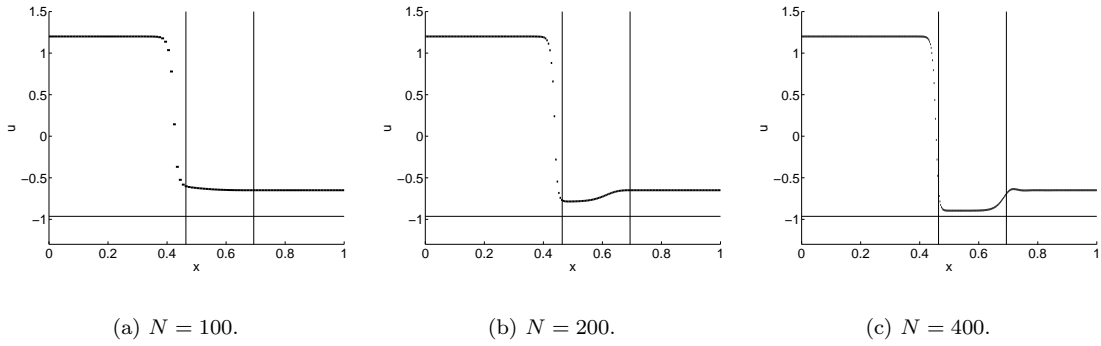


FIGURE 3. Piecewise constant approximations for the local problem (1), (7) after a grid refinement. The thin lines indicate the shock positions and the middle state  $u_m$  at  $t = 0.3$ .

$\varepsilon$	$\ u_{h,local}^\varepsilon - u^0\ _{L^1(0,1)}$	
	$p = 2$	$p = 3$
0.016	1.1383e-01	1.1561e-01
0.008	5.7521e-02	5.7988e-02
0.004	2.8960e-02	2.8781e-02
0.002	1.4819e-02	1.4059e-02
0.001	1.8562e-02	7.6740e-03

FIGURE 4.  $L^1$ -error between  $u_{h,local}^\varepsilon$  and the limit solution  $u^0$  at the time  $t = 0.3$ , where  $u_{h,local}^\varepsilon$  comes out of the local LDG-scheme (16).

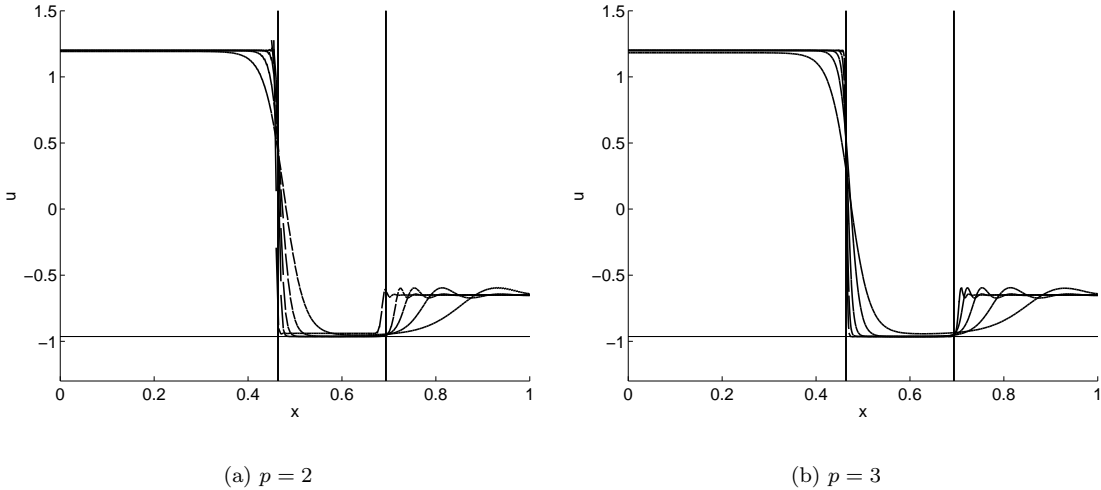


FIGURE 5. Local piecewise linear and quadratic solutions  $u_{h,local}^\varepsilon(\cdot, t = 0.3)$  on  $N = 200$  cells for various  $\varepsilon$ . The thin lines indicate the shock positions and the middle state  $u_m$  at  $t = 0.3$ .

in this example. We use the same setting as in Testproblem 1a but start with the initial function

$$u_0(x) = \frac{1}{2} \left( u_l + u_r - (u_l - u_r) \tanh \left( \frac{u_l - u_r}{2\varepsilon\sqrt{2\lambda}} (x - 0.2) \right) \right),$$

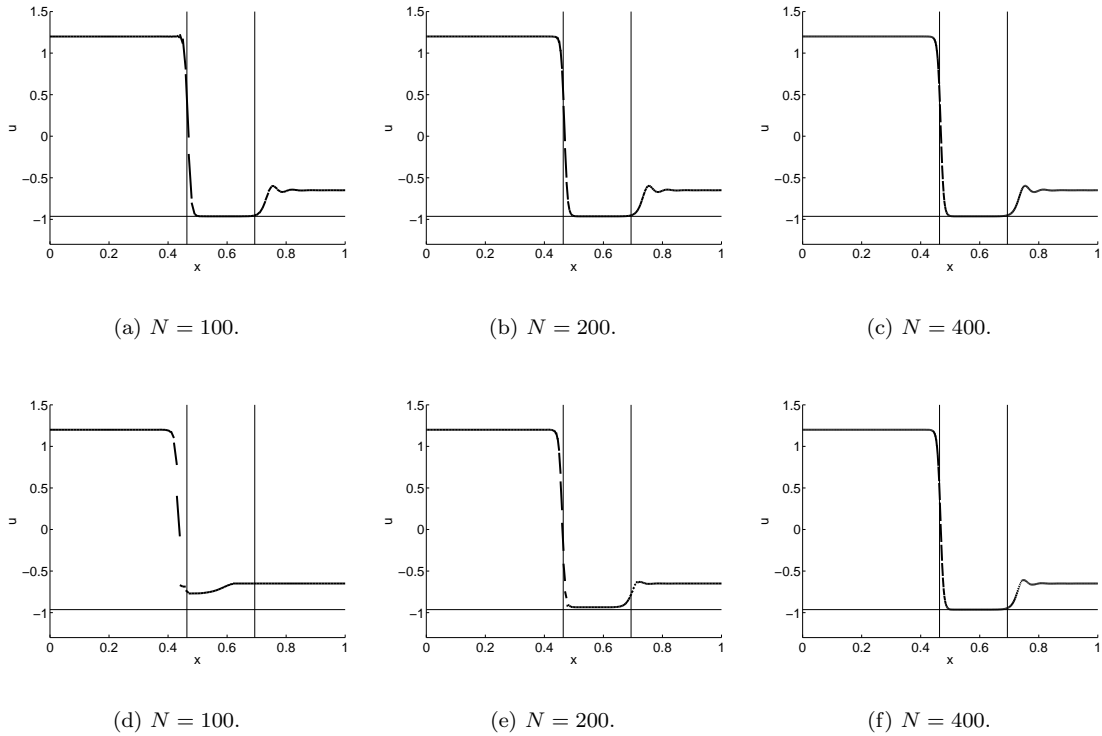


FIGURE 6. Piecewise linear approximations for the local problem (1), (7) on various grids. We used no slope-limiter in the upper row resp. the Minmod-slope-limiter in the lower row. The thin lines indicate the shock positions and the middle state  $u_m$  at  $t = 0.3$ .

where we have  $u_l = 1.2$  and  $u_r = -u_l + \frac{1}{3}\sqrt{\frac{2}{\lambda}} \approx -0.964$ . Then the exact solution for (1), (2) with the local right hand side (7) is the travelling wave  $u(x, t) = u_0(x - st)$  with the speed  $s = \frac{u_r^3 - u_m^3}{u_r - u_m} \approx 1.213$  (see [18]). Fig. 7 shows the piecewise constant numerical solutions for the local LDG-scheme (16) on an equidistant partition  $\{I_j\}_{j=1, \dots, N}$ ,  $N = 400$ , at the time  $t = 0.2$ . Instead of the travelling wave solution the Upwind- and local Lax-Friedrichs-results seem to produce another spurious solution consisting of a middle state and a rarefaction wave. Not so with the Tadmor-experiment where the solution represents the travelling wave with the correct speed. Let us mention that the solutions for all three flux choices tend to the correct travelling wave solution if we use finer grids or increase  $p$ .

**Testproblem 3.** In a last example we slightly change the parameter  $\lambda$  that couples the diffusion and dispersion terms in (7) and (8) to  $\lambda = 1$ . As already mentioned the structure of the solution sensitively depends on this parameter. For the initial datum

$$u_0(x) = \begin{cases} u_l = 1.2 & : x \leq 0.1, \\ u_r = -0.8 & : x > 0.1 \end{cases}$$

the limit solution  $u^0$  no longer has a shock-shock- but a shock-rarefaction-shape (see [18]). Here the shock has the speed  $s = \frac{u_l^3 - u_m^3}{u_l - u_m} \approx 1.097$  and the rarefaction evolves between the middle state  $u_m = -u_l + \frac{1}{3}\sqrt{\frac{2}{\lambda}} \approx -0.729$  and the right state  $u_r = -0.8$ .

Fig. 8 shows the numerical results  $u_h \in \mathcal{V}_h^p$  for  $p = 1, 2, 3$  (piecewise constant, linear, quadratic) on an equidistant partition  $\{I_j\}_{j=1, \dots, N}$  of  $[0, 1]$  consisting of  $N = 200$  cells. We set  $\varepsilon = 0.004$ .

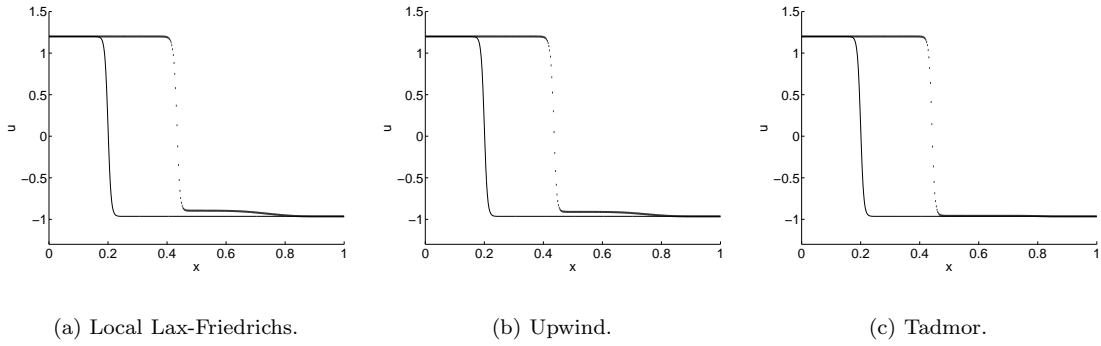


FIGURE 7. Travelling wave solutions for the local problem (1), (7) for various numerical flux functions at  $t = 0.2$ . The thin lines indicate the initial function.

Again we compare the results for the local LDG-scheme (16) (see Fig. 8, upper row) and the two variants of the non-local LDG-scheme (21) resp. (25) (see Fig. 8, middle resp. lower row). The positions of the shock, the front and the end of the rarefaction wave as well as the middle state  $u_m$  for the limit solution are drawn by thin lines in Fig. 8. Similar as before in the shock-shock-example the source-like non-local variant of the LDG-scheme (25) gives the best numerical solutions, i.e., even in the piecewise constant case the middle state and rarefaction wave clearly evolve.

### 3. The Local and Non-Local Elasticity System

#### 3.1. Phase Transitions and the Elasticity System

In this last section we consider the Cauchy problem for the one-dimensional system of elasticity (12). In the introduction we defined phases for this system. Let us furthermore note that the eigenvalues of the Jacobian of the flux  $f(w, v) = (-v, -\sigma(w))^T$  in (12) are given by  $\mp\sqrt{\sigma'(w)}$ ,  $w \in \mathbb{R}$ , so that the system, for  $\varepsilon \equiv 0$ , is only hyperbolic in the two distinct phases but altogether an instance of a mixed hyperbolic-elliptic system. While such systems are widely used to describe phase transition in solids (cf. [13]) on the other hand all classical existence theorems for purely hyperbolic systems fail. For the derivation of the local and in particular the non-local variant in (12) as well as the modeling background we refer to e.g. [15, 17].

In the numerical experiments we will investigate the time-asymptotics for solutions of (12). For  $t \rightarrow \infty$  we assume that the process reaches an equilibrium configuration, more specifically it is expected that the solution is a minimizer of the total stored energy

$$(34) \quad E_{local}^\varepsilon[w] := E^0[w] + \frac{1}{2}\lambda\varepsilon^2 \int_{\mathbb{R}} |w_x(x)|^2 dx,$$

in the local case and

$$(35) \quad E_{global}^\varepsilon[w] := E^0[w] + \frac{1}{4}\lambda\gamma \int_{\mathbb{R}} \int_{\mathbb{R}} \Phi_\varepsilon(x-y) |w(x) - w(y)|^2 dy dx,$$

in the non-local case. In (34) and (35)  $w$  is a sufficiently regular function and  $E^0$  is defined through

$$(36) \quad E^0[w] = \int_{\mathbb{R}} W(w(x)) dx, \quad W'(w) = \sigma(w).$$

Note that due to the non-monotone shape of  $\sigma$  the function  $W$  has the double-well form which leads to many inhomogenous minimizers of (36) even if the total mass is assumed to be fixed. From the purely mathematical point of view the second term in (34) regularizes possible minimizers but also penalizes the occurrence of phase interfaces. We can assume that the solutions of (12) converge for  $t \rightarrow \infty$  to a configuration with a minimal number of phase changes.

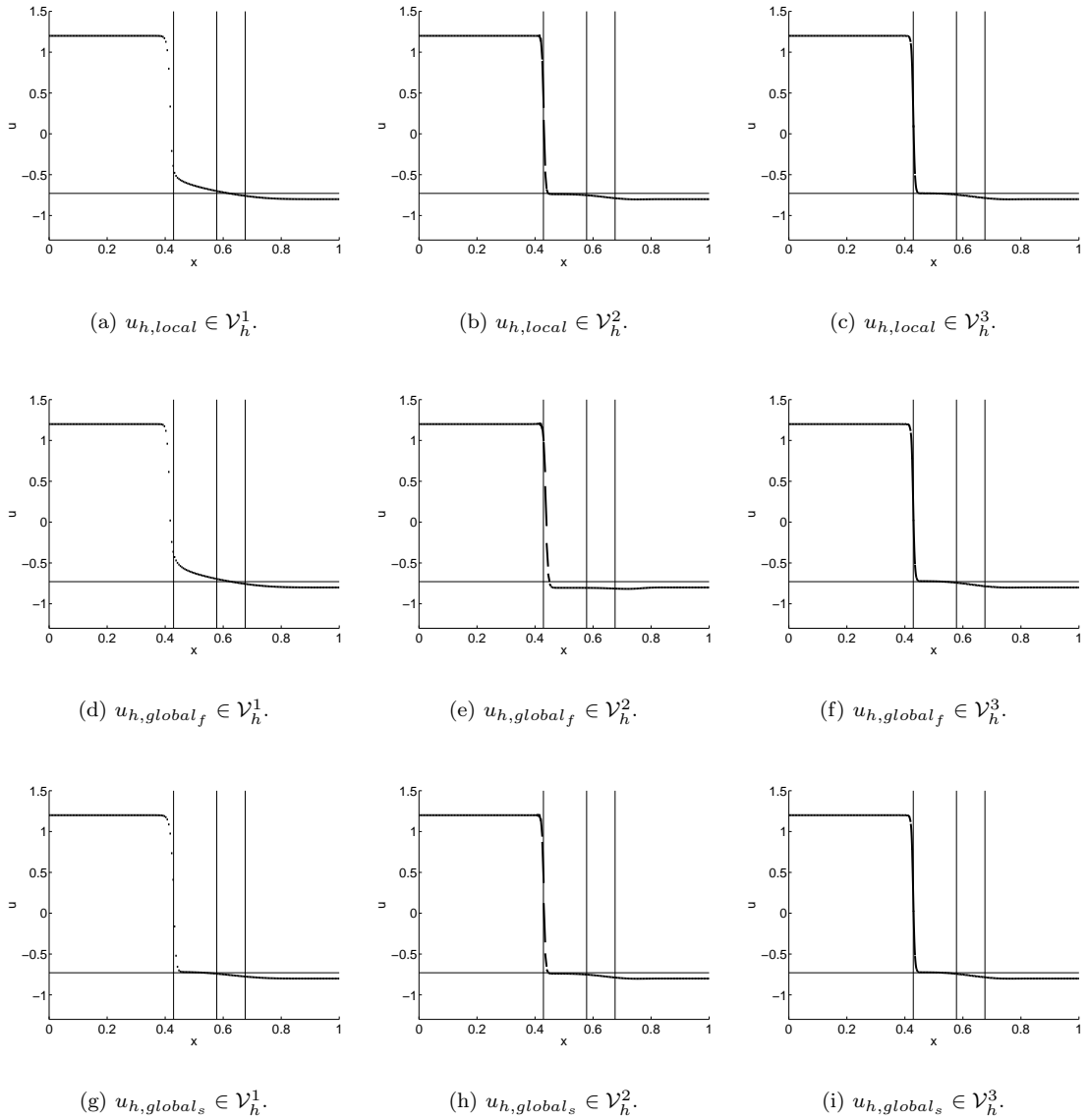


FIGURE 8. Numerical solutions of (1) with (7) (upper row) or (8) (middle and lower row) on an equidistant partition  $\{I_j\}_{j=1,\dots,N}$  ( $N = 200$ ) of  $[0, 1]$  at the time  $t = 0.3$ .

The limit solution  $u^0$  consists of an undercompressive shock and a rarefaction wave. The thin lines indicate the positions of the shock, the front and the end of the rarefaction wave as well as the middle state at  $t = 0.3$ .

The penalizing effect of the second term in (35) depends on the properties of the kernel  $\Phi$  ( $\Phi_\varepsilon$  always given as in (10)). If we choose  $\Phi$  as the non-negative function

$$(37) \quad \Phi^\tau(x) = \begin{cases} \frac{\exp(\tau^2/(x^2-\tau^2))}{\int_{-\tau}^{\tau} \exp(\tau^2/(y^2-\tau^2)) dy} & : x \in (-\tau, \tau), \\ 0 & : \text{otherwise} \end{cases}$$

for some  $\tau > 0$  we recover the strictly penalizing situation and expect again a complete phase separation for the time-asymptotic configuration. The situation is drastically different if we allow for kernels which become negative somewhere (still the physical assumptions (11) are supposed to

hold). Then the end state could still involve configurations with more than the minimal number of phase changes. Not completely non-negative kernels have been suggested by Ren&Truskinovsky [15]. We note that there is no such flexibility in the local modeling. When we allow for such type of kernels automatically the question arises how many phase changes show up in the asymptotic limit. We introduce a new family of kernels  $\{\Phi^\tau\}_{\tau>0}$  which enables to tune this number in a controlled way as our numerical experiments will show. They are given by even functions for which

$$(38) \quad \Phi^\tau(x) = \begin{cases} -\frac{800}{41\tau^2}(x - \frac{9}{20}\tau) & : x \in [0, \frac{29}{40}\tau], \\ \frac{800}{41\tau^2}(x - \tau) & : x \in (\frac{29}{40}\tau, \tau], \\ 0 & : x > \tau. \end{cases}$$

holds (see Fig. 11, upper row). We observe that the kernel penalizes phase transitions on a small scale while they benefit on a larger distance.

### 3.2. Formulation of the LDG-Scheme

Let us perform the LDG-discretization for the one-dimensional system of elasticity (12). As described in Sect. 2 we introduce new variables to handle the diffusive and dispersive terms in (12). In the local variant in (12) we consider the system (skipping again the index  $\varepsilon$ )

$$(39) \quad \begin{aligned} w_t - v_x &= 0, \\ v_t - (\sigma(w) + \varepsilon r - \lambda \varepsilon^2 p)_x &= 0, \\ r - v_x &= 0, \\ q - w_x &= 0, \\ p - q_x &= 0, \end{aligned}$$

in the non-local variant merely

$$(40) \quad \begin{aligned} w_t - v_x &= 0, \\ v_t - (\sigma(w) + \varepsilon r - \lambda \gamma (\Phi_\varepsilon * w - w))_x &= 0, \\ r - v_x &= 0. \end{aligned}$$

Another possibility to derive a non-local LDG-scheme arises if we first rewrite the convolution term  $D^\varepsilon[w]_x = D^\varepsilon[q]$  where  $q = w_x$ , i.e., if we discretize the system

$$(41) \quad \begin{aligned} w_t - v_x &= 0, \\ v_t - (\sigma(w) + \varepsilon r)_x + \lambda \gamma (\Phi_\varepsilon * q - q) &= 0, \\ r - v_x &= 0, \\ q - w_x &= 0. \end{aligned}$$

Since we got better numerical results for the rewritten convolution term in Sect. 2 we will use the source-like variant of LDG-scheme, i.e., the LDG-scheme for (41), in the numerical experiments at the end of this section. To obtain LDG-discretizations for all of these three reformulations the techniques of Sect. 2.1 can be adopted. Again we have to introduce numerical flux functions to approximate the analytical fluxes at the cell boundaries  $x_{j\pm 1/2}$ . In the numerical examples below we choose Tadmor's flux for  $\tilde{f}$  and central fluxes as in (19) for all the remaining numerical flux functions in the LDG-schemes. To detect Tadmor's flux (see also (18)) we first change the

unknowns  $(w, v)^T$  into  $(\sigma(w), v)^T = \nabla \eta(w, v)$  for the entropy  $\eta(w, v) = W(w) + \frac{v^2}{2}$  and obtain

$$\begin{aligned}
\tilde{f} \left( \begin{pmatrix} w_h(x_{j+1/2}^-, t) \\ v_h(x_{j+1/2}^-, t) \end{pmatrix}, \begin{pmatrix} w_h(x_{j+1/2}^+, t) \\ v_h(x_{j+1/2}^+, t) \end{pmatrix} \right) &= \tilde{g} \left( \begin{pmatrix} \sigma(w_h(x_{j+1/2}^-, t)) \\ v_h(x_{j+1/2}^-, t) \end{pmatrix}, \begin{pmatrix} \sigma(w_h(x_{j+1/2}^+, t)) \\ v_h(x_{j+1/2}^+, t) \end{pmatrix} \right) \\
&= \int_0^1 g \left( \begin{pmatrix} \sigma(w_h(x_{j+1/2}^-, t)) \\ v_h(x_{j+1/2}^-, t) \end{pmatrix} + s \begin{pmatrix} \sigma(w_h(x_{j+1/2}^+, t)) - \sigma(w_h(x_{j+1/2}^-, t)) \\ v_h(x_{j+1/2}^+, t) - v_h(x_{j+1/2}^-, t) \end{pmatrix} \right) ds \\
(42) \quad &= - \int_0^1 \begin{pmatrix} v_h(x_{j+1/2}^-, t) \\ \sigma(w_h(x_{j+1/2}^-, t)) \end{pmatrix} + s \begin{pmatrix} v_h(x_{j+1/2}^+, t) - v_h(x_{j+1/2}^-, t) \\ \sigma(w_h(x_{j+1/2}^+, t)) - \sigma(w_h(x_{j+1/2}^-, t)) \end{pmatrix} ds \\
&= - \frac{1}{2} \begin{pmatrix} v_h(x_{j+1/2}^-, t) + v_h(x_{j+1/2}^+, t) \\ \sigma(w_h(x_{j+1/2}^-, t)) + \sigma(w_h(x_{j+1/2}^+, t)) \end{pmatrix}.
\end{aligned}$$

### 3.3. Discrete Energy Estimate

It is easy to check that classical solutions  $(w^\varepsilon, v^\varepsilon)$  of (12), (13) satisfy the energy inequality

$$(43) \quad \frac{d}{dt} \left( E_{local/global}^\varepsilon[w^\varepsilon(\cdot, t)] + \frac{1}{2} \int_{\mathbb{R}} (v^\varepsilon(x, t))^2 dx \right) \leq 0$$

for all  $t \geq 0$  with (34) resp. (35). The relation (43) is nothing but a form of the Clausius-Duhem inequality for 1D-elasticity. We use this property of the exact solution to validate our numerical results. Indeed the total energy (potential energy + kinetic energy) of the numerical solution decreases almost monotonically in time in an example at the end of this section. Unfortunately no analytical energy result exists for the solutions of the LDG-schemes in the case of (39) or (41) up to our knowledge. But we have a discrete (slightly differing) counterpart to (43) for the flux-like LDG-scheme of the non-local rewritten system of elasticity (40). Thus consider the LDG-scheme of (40), i.e.,

$$\begin{aligned}
(44) \quad &\int_{I_j} w_{h,t}(x, t) \phi_h(x) dx + \int_{I_j} v_h(x, t) \phi_{h,x}(x) dx = \tilde{v}_{j+1/2} \phi_h(x_{j+1/2}^-) - \tilde{v}_{j-1/2} \phi_h(x_{j-1/2}^+), \\
&\int_{I_j} v_{h,t}(x, t) \phi_h(x) dx + \int_{I_j} (\sigma(w_h(x, t)) + \varepsilon r_h(x, t) - \lambda \gamma (\overline{[\Phi_\varepsilon * w_h(\cdot, t)]}(x) - w_h(x, t))) \phi_{h,x}(x) dx \\
&= \tilde{\sigma}_{j+1/2} \phi_h(x_{j+1/2}^-) - \tilde{\sigma}_{j-1/2} \phi_h(x_{j-1/2}^+) \\
&\quad + \varepsilon \tilde{r}_{j+1/2} \phi_h(x_{j+1/2}^-) - \varepsilon \tilde{r}_{j-1/2} \phi_h(x_{j-1/2}^+) \\
&\quad - \lambda \gamma \widetilde{[\Phi_\varepsilon * w_h(\cdot, t)]}(x_{j+1/2}) \phi_h(x_{j+1/2}^-) + \lambda \gamma \widetilde{[\Phi_\varepsilon * w_h(\cdot, t)]}(x_{j-1/2}) \phi_h(x_{j-1/2}^+) \\
&\quad + \lambda \gamma \tilde{w}_{j+1/2} \phi_h(x_{j+1/2}^-) - \lambda \gamma \tilde{w}_{j-1/2} \phi_h(x_{j-1/2}^+), \\
&\int_{I_j} r_h(x, t) \phi_h(x) dx + \int_{I_j} v_h(x, t) \phi_{h,x}(x) dx = \tilde{v}_{j+1/2} \phi_h(x_{j+1/2}^-) - \tilde{v}_{j-1/2} \phi_h(x_{j-1/2}^+)
\end{aligned}$$

for all  $\phi_h \in \mathcal{V}_h^p$ ,  $j \in \mathbb{Z}$  and  $t \geq 0$ . Here we abbreviate

$$\begin{aligned}
\tilde{w}_{j+1/2} &:= \tilde{w}(w_h(x_{j+1/2}^-, t), w_h(x_{j+1/2}^+, t)), \\
\tilde{v}_{j+1/2} &:= \tilde{v}(v_h(x_{j+1/2}^-, t), v_h(x_{j+1/2}^+, t)), \\
\tilde{r}_{j+1/2} &:= \tilde{r}(r_h(x_{j+1/2}^-, t), r_h(x_{j+1/2}^+, t)), \\
\tilde{\sigma}_{j+1/2} &:= \tilde{\sigma}(w_h(x_{j+1/2}^-, t), w_h(x_{j+1/2}^+, t))
\end{aligned}$$

for some numerical flux functions  $\tilde{w}, \tilde{v}, \tilde{r}, \tilde{\sigma} : \mathbb{R}^2 \rightarrow \mathbb{R}$ . The notations  $\overline{[\Phi_\varepsilon * w_h]}$  and  $\widetilde{[\Phi_\varepsilon * w_h]}$  in (44) are interpreted as follows.



Consider a fixed equidistant grid with grid size  $h$ . For the given kernel  $\Phi$  let  $\Phi^h$  be a symmetric, piecewise constant approximation such that

$$\int_{\mathbb{R}} \Phi^h(x) dx = 1$$

is still fulfilled. In detail we require that  $\Phi^h$  is constant for all  $x \in (\frac{2k-1}{2}h, \frac{2k+1}{2}h)$ ,  $k \in \mathbb{Z}$  (see Fig. 9).

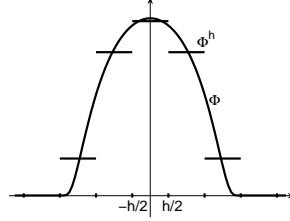


FIGURE 9. Piecewise constant approximation  $\Phi^h$  for the kernel  $\Phi$ .

Then with this approximation  $\Phi^h$  we substitute the quadrature formula

$$\overline{[\Phi_\varepsilon * w_h(\cdot, t)]}(x) := \sum_{k \in \mathbb{Z}} h \Phi_\varepsilon^h(x - x_k) w_h(x_k, t)$$

in (44) for the original convolution integral  $[\Phi_\varepsilon * w_h(\cdot, t)](x) = \int_{\mathbb{R}} \Phi_\varepsilon(x - y) w_h(y, t) dy$ . Here  $x_k$  denotes the cell midpoint of  $I_k$  and we have  $\Phi_\varepsilon^h(x) = \frac{1}{\varepsilon} \Phi^h(\frac{x}{\varepsilon})$  for all  $x \in \mathbb{R}$ . Furthermore let us define

$$(45) \quad \widetilde{[\Phi_\varepsilon * w_h(\cdot, t)]}(x_{j+1/2}) := \frac{1}{2} \left( \overline{[\Phi_\varepsilon * w_h(\cdot, t)]}(x_{j+1/2}^-) + \overline{[\Phi_\varepsilon * w_h(\cdot, t)]}(x_{j+1/2}^+) \right).$$

Now we have the following discrete energy estimate for the solutions of (44).

**Theorem 3.1** (Discrete Energy Estimate). *Let  $w_h, v_h \in \mathcal{V}_h^1$  be the piecewise constant solutions of (44) on an equidistant grid and*

$$|w_h(x, t)|, |v_h(x, t)|, |r_h(x, t)| \rightarrow 0 \quad \text{for } x \rightarrow \pm\infty, t \geq 0$$

be satisfied. Furthermore let the numerical fluxes be (45) and central fluxes

$$(46) \quad \tilde{w}/\tilde{v}/\tilde{r}(a, b) = \frac{1}{2}(a + b), \quad \tilde{\sigma}(a, b) = \frac{1}{2}(\sigma(a) + \sigma(b)).$$

Then

$$(47) \quad \frac{d}{dt} \int_{\mathbb{R}} \left( W(w_h(x, t)) + \frac{v_h^2(x, t)}{2} + \frac{1}{4} \lambda \gamma \sum_{k \in \mathbb{Z}} h \Phi_\varepsilon^h(x - x_k) [w_h(x_k, t) - w_h(x, t)]^2 \right) dx \leq 0$$

holds true for all  $t \geq 0$ .

Note that (46) includes nothing but Tadmor's flux  $\tilde{f} = (-\tilde{v}, -\tilde{\sigma})^T$  (see (42)) for the original flux  $f = (-v, -\sigma(w))^T$  of (12).

*Proof.* Similar to the proofs of Theorem 2.1 and 2.3 we choose special test functions  $\phi_h$  in the LDG-scheme (44) and add up all gained equations. In detail we consider for  $t \geq 0$  fixed  $\phi_h = \sigma(w_h(\cdot, t)) - \lambda \gamma (\overline{[\Phi_\varepsilon * w_h(\cdot, t)]} - w_h(\cdot, t))$  in the first,  $\phi_h = v_h(\cdot, t)$  in the second and  $\phi_h = \varepsilon r_h(\cdot, t)$  in the third equation of (44). Note that especially  $\phi_h = \sigma(w_h(\cdot, t))$  and  $\phi_h = \overline{[\Phi_\varepsilon * w_h(\cdot, t)]}$  are suitable test functions, i.e., they are piecewise constant. Then we obtain

$$\begin{aligned} & \frac{d}{dt} \int_{I_j} \left( W(w_h(x, t)) + \frac{v_h^2(x, t)}{2} \right) dx \\ & - \lambda \gamma \int_{I_j} \left( \overline{[\Phi_\varepsilon * w_h(\cdot, t)]}(x) - w_h(x, t) \right) w_{h,t}(x, t) dx + g_{j+1/2} - g_{j-1/2} = -\varepsilon \int_{I_j} r_h^2(x, t) dx \end{aligned}$$

with

$$\begin{aligned}
g_{j+1/2} &= g(w_h(x_{j+1/2}^-, t), w_h(x_{j+1/2}^+, t), v_h(x_{j+1/2}^-, t), v_h(x_{j+1/2}^+, t), r_h(x_{j+1/2}^-, t), r_h(x_{j+1/2}^+, t)) \\
&:= v_h(x_{j+1/2}^-, t)\sigma(w_h(x_{j+1/2}^-, t)) - \tilde{v}(v_h(x_{j+1/2}^-, t), v_h(x_{j+1/2}^+, t))\sigma(w_h(x_{j+1/2}^-, t)) \\
&\quad - \tilde{\sigma}(w_h(x_{j+1/2}^-, t), w_h(x_{j+1/2}^+, t))v_h(x_{j+1/2}^-, t) \\
&\quad + \varepsilon \left( v_h(x_{j+1/2}^-, t)r_h(x_{j+1/2}^-, t) - \tilde{v}(v_h(x_{j+1/2}^-, t), v_h(x_{j+1/2}^+, t))r_h(x_{j+1/2}^-, t) \right. \\
&\quad \quad \left. - \tilde{r}(r_h(x_{j+1/2}^-, t), r_h(x_{j+1/2}^+, t))v_h(x_{j+1/2}^-, t) \right) \\
&\quad + \lambda\gamma \left( v_h(x_{j+1/2}^-, t)w_h(x_{j+1/2}^-, t) - \tilde{v}(v_h(x_{j+1/2}^-, t), v_h(x_{j+1/2}^+, t))w_h(x_{j+1/2}^-, t) \right. \\
&\quad \quad \left. - \tilde{w}(w_h(x_{j+1/2}^-, t), w_h(x_{j+1/2}^+, t))v_h(x_{j+1/2}^-, t) \right) \\
&\quad - \lambda\gamma \left( v_h(x_{j+1/2}^-, t)\overline{[\Phi_\varepsilon * w_h(\cdot, t)]}(x_{j+1/2}^-) \right. \\
&\quad \quad - \tilde{v}(v_h(x_{j+1/2}^-, t), v_h(x_{j+1/2}^+, t))\overline{[\Phi_\varepsilon * w_h(\cdot, t)]}(x_{j+1/2}^-) \\
&\quad \quad \left. - \widetilde{[\Phi_\varepsilon * w_h(\cdot, t)]}(x_{j+1/2}^-)v_h(x_{j+1/2}^-, t) \right).
\end{aligned}$$

Note that there are no other terms left after summation of the three equations in (44) if we use the central fluxes (45), (46). Now if we add up over all intervals  $\{I_j\}_{j \in \mathbb{Z}}$  the energy inequality (47) follows if we observe that

$$\begin{aligned}
& - \int_{\mathbb{R}} \left( \overline{[\Phi_\varepsilon * w_h(\cdot, t)]}(x) - w_h(x, t) \right) w_{h,t}(x, t) \, dx \\
&= - \sum_{j \in \mathbb{Z}} \int_{I_j} \left( \left\{ \sum_{k \in \mathbb{Z}} h\Phi_\varepsilon^h(x - x_k)w_h(x_k, t) \right\} - w_h(x, t) \right) w_{h,t}(x, t) \, dx \\
&= - \sum_{j \in \mathbb{Z}} h \left( \sum_{k \in \mathbb{Z}} h\Phi_\varepsilon^h(x_j - x_k)[w_h(x_k, t) - w_h(x_j, t)] \right) w_{h,t}(x_j, t) \\
&= \frac{1}{2} \sum_{j \in \mathbb{Z}} h \sum_{k \in \mathbb{Z}} h\Phi_\varepsilon^h(x_j - x_k)[w_h(x_j, t) - w_h(x_k, t)]w_{h,t}(x_j, t) \\
&\quad - \frac{1}{2} \sum_{j \in \mathbb{Z}} h \sum_{k \in \mathbb{Z}} h\Phi_\varepsilon^h(x_j - x_k)[w_h(x_k, t) - w_h(x_j, t)]w_{h,t}(x_j, t) \\
&= \frac{1}{4} \frac{d}{dt} \sum_{j \in \mathbb{Z}} h \sum_{k \in \mathbb{Z}} h\Phi_\varepsilon^h(x_j - x_k)[w_h(x_k, t) - w_h(x_j, t)]^2 \\
&= \frac{1}{4} \frac{d}{dt} \int_{\mathbb{R}} \sum_{k \in \mathbb{Z}} h\Phi_\varepsilon^h(x - x_k)[w_h(x_k, t) - w_h(x, t)]^2 \, dx
\end{aligned}$$

holds true. Here we used  $\overline{[\Phi_\varepsilon * w_h]}|_{I_j} = \text{const}$  as well as  $\sum_{k \in \mathbb{Z}} h\Phi_\varepsilon^h(x_j - x_k) = 1$  for all  $j \in \mathbb{Z}$ , thanks to the special form of  $\Phi^h$ .  $\square$

### 3.4. Numerical Experiments

**Testproblem 1.** As a first example we consider the one-dimensional system of elasticity (12) with the viscosity and capillarity parameters  $\varepsilon = 0.01$  and  $\lambda = 10$  and start with

$$w_0(x) = \begin{cases} 1.2 & : x \in [1/8, 1/4], x \in [1/2, 7/8] \\ -1.2 & : \text{otherwise} \end{cases}, \quad v_0 \equiv 0 \quad \text{for all } x \in \mathbb{R}.$$

In the non-local version of (12) we take the kernel functions  $\Phi^\tau$  as in (37) with either  $\tau = 1$  or  $\tau = 10$ .

In Fig. 10 the respective local and non-local solutions are shown at different times. To shorten

the resulting figures we only look for piecewise quadratic solutions, i.e.,  $w_h, v_h \in \mathcal{V}_h^3$ . Let us mention again that we used the source-like LDG-scheme obtained by (41) in the non-local case. As expected the occurrence of phase interfaces is penalized and thus the number of phase changes decreases from 4 to 2. Note that in the non-local model with  $\tau = 10$  the width of the transition layer is even smaller than in both other cases.

In [6] the authors report on the occurrence of spurious oscillations close to phase boundaries (in 2D-computations). This is a typical problem for phase separation processes and spurious effects would also be present if we would discretize (12), (13) with a standard finite difference scheme using e.g. the Lax-Friedrichs flux as the numerical flux. It is a remarkable property of the LDG-approach that no such spurious oscillations are observed in our experiments.

**Testproblem 2.** In a last experiment we are interested in numerical solutions which come out of the non-local version of (12), where we also permit the kernel function  $\Phi$  to have negative parts, i.e., we consider (38) with  $\tau \in \{3, 5, 10\}$  sketched in the upper row of Fig. 11. As parameters in (12) we choose  $\varepsilon = 0.01$ ,  $\lambda = 1$ ,  $\gamma = 1$  and as initial data

$$w_0(x) = \begin{cases} 1.2 & : x \in [0, 1/2] \\ -1.2 & : \text{otherwise} \end{cases}, \quad v_0 \equiv 0 \quad \text{for all } x \in \mathbb{R}.$$

Fig. 11 shows the piecewise quadratic approximations obtained with the LDG-scheme of (41) equipped with a limiter proposed by Dolejsi [7]. The three columns in Fig. 11 display the results for the three different choices of  $\tau$  in the kernel  $\Phi^\tau$ . Obviously we get the more number of phase interfaces the smaller  $\tau$  is. For larger times  $t$  the velocity  $v_h$  more and more slows down, i.e., the configuration tends towards a static equilibrium. This is also underlined in Fig. 12 by the temporal development of the energy

$$F_{global}^\varepsilon[w_h, v_h] := \int_0^1 \left( W(w_h(x, t)) + \frac{v_h^2(x, t)}{2} + \frac{1}{4} \lambda \gamma \int_{\mathbb{R}} \Phi_\varepsilon^\tau(x - y) |w_h(x, t) - w_h(y, t)|^2 dy \right) dx.$$

## References

- [1] C. Chalons and P.G. LeFloch, A fully discrete scheme for diffusive-dispersive conservation laws, *Numer. Math.* 89 (2001), no. 3, 493–509.
- [2] B. Cockburn, Discontinuous Galerkin methods. *ZAMM Z. Angew. Math. Mech.* 83 (2003), no. 11, 731-754.
- [3] B. Cockburn, G.E. Karniadakis, and C.-W. Shu (eds.), *Discontinuous Galerkin methods*, Lect. Notes Comput. Sci. Eng. 11, Springer, Berlin (2000).
- [4] B. Cockburn and C.-W. Shu, The Runge-Kutta local projection  $P^1$ -discontinuous-Galerkin finite element method for scalar conservation laws. *RAIRO Modél. Math. Anal. Numér.* 25 (1991), no. 3, 337-361.
- [5] B. Cockburn and C.-W. Shu, The local discontinuous Galerkin finite element method for convection-diffusion systems, *SIAM J. Numer. Anal.* 35 (1998) 2440-2463.
- [6] F. Coquel, D. Diehl, C. Merkle, and C. Rohde, Sharp and diffuse interface methods for phase transition problems in liquid-vapour flows. *Numerical methods for hyperbolic and kinetic problems*, IRMA Lect. Math. Theor. Phys., 7, Eur. Math. Soc., Zürich (2005), 239-270.
- [7] V. Dolejsi, On the Discontinuous Galerkin Method for the Numerical Solution of the Euler and the Navier-Stokes Equations. *Int. J. Numer. Methods Fluids* (submitted). Also The Preprint Series of the School of Mathematics, Charles University Prague, No. MATH-KNM-2002/2 (2002).
- [8] J.L. Ericksen, Equilibrium of bars. *J. Elasticity* 5 (1975), 191-201.
- [9] B.T. Hayes and P.G. LeFloch, Non-classical shocks and kinetic relations: scalar conservation laws. *Arch. Rational Mech. Anal.* 139 (1997), no. 1, 1-56.
- [10] B.T. Hayes and P.G. LeFloch, Nonclassical shocks and kinetic relations: strictly hyperbolic systems. *SIAM J. Math. Anal.* 31 (2000), no. 5, 941-991.
- [11] P.G. LeFloch, *Hyperbolic systems of conservation laws. The theory of classical and nonclassical shock waves.* Lectures in Mathematics ETH Zürich. Basel: Birkhäuser (2002), 294 pp.
- [12] P.G. LeFloch, J.M. Mercier, and C. Rohde, Fully discrete, entropy conservative schemes of arbitrary order. *SIAM J. Numer. Anal.* 40 (2002), no. 5, 1968-1992.
- [13] R.D. James, The propagation of phase boundaries in elastic bars. *Arch. Rational Mech. Anal.* 73 (1980), no. 2, 125-158.
- [14] D. Levy, C.-W. Shu, and J. Yan, Local discontinuous Galerkin methods for nonlinear dispersive equations. *J. Comput. Phys.* 196 (2004), no. 2, 751-772.
- [15] X. Ren and L. Truskinovsky, Finite scale microstructures in nonlocal elasticity, *J. Elasticity* 59 (2000), 319-355.

- [16] C. Rohde, Scalar conservation laws with mixed local and nonlocal diffusion-dispersion terms. *SIAM J. Math. Anal.* 37 (2005), no. 1, 103-129.
- [17] C. Rohde, Phase transitions and sharp-interface limits for the 1d-elasticity system with non-local energy. *Interfaces Free Bound.* 7 (2005), no. 1, 107-129.
- [18] D. Jacobs, B. McKinney, and M. Shearer, Travelling wave solutions of the modified Korteweg-de Vries-Burgers equation. *J. Differential Equations* 116 (1995), no. 2, 448-467.
- [19] E. Tadmor, Entropy stability theory for difference approximations of nonlinear conservation laws and related time dependent problems. *Acta Numerica* (2003), 451-512.
- [20] E. Tadmor, The numerical viscosity of entropy stable schemes for systems of conservation laws. *Math. Comp.* 49 (1987), no. 179, 91-103.
- [21] J. Yan and C.-W. Shu, A local discontinuous Galerkin method for KdV type equations. *SIAM J. Numer. Anal.* 40 (2002), no. 2, 769-791.

FACHBEREICH MATHEMATIK - IANS  
UNIVERSITÄT STUTTGART  
PFAFFENWALDRING 57  
D-70569 STUTTGART  
GERMANY

*E-mail address:* Jenny.Haink|Christian.Rohde@mathematik.uni-stuttgart.de

Jenny Haink  
Pfaffenwaldring 57  
70569 Stuttgart  
Germany

**E-Mail:** Jenny.Haink@mathematik.uni-stuttgart.de

**WWW:** <http://www.ians.uni-stuttgart.de/am/Haink/>

Christian Rohde  
Pfaffenwaldring 57  
70569 Stuttgart  
Germany

**E-Mail:** Christian.Rohde@mathematik.uni-stuttgart.de

**WWW:** <http://www.ians.uni-stuttgart.de/am/Rohde/>

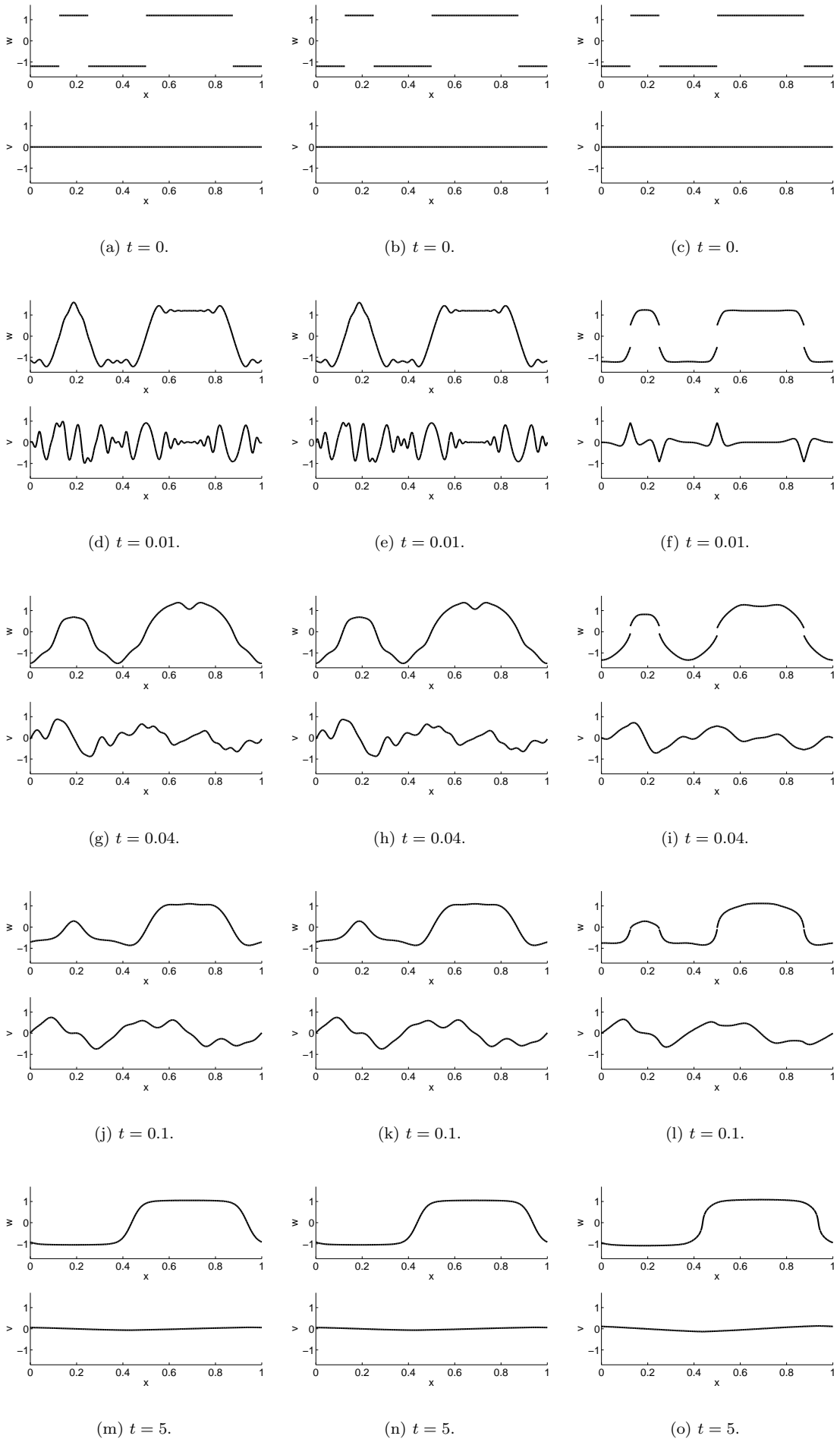


FIGURE 10. Phase separation problem for the local (left column) and non-local

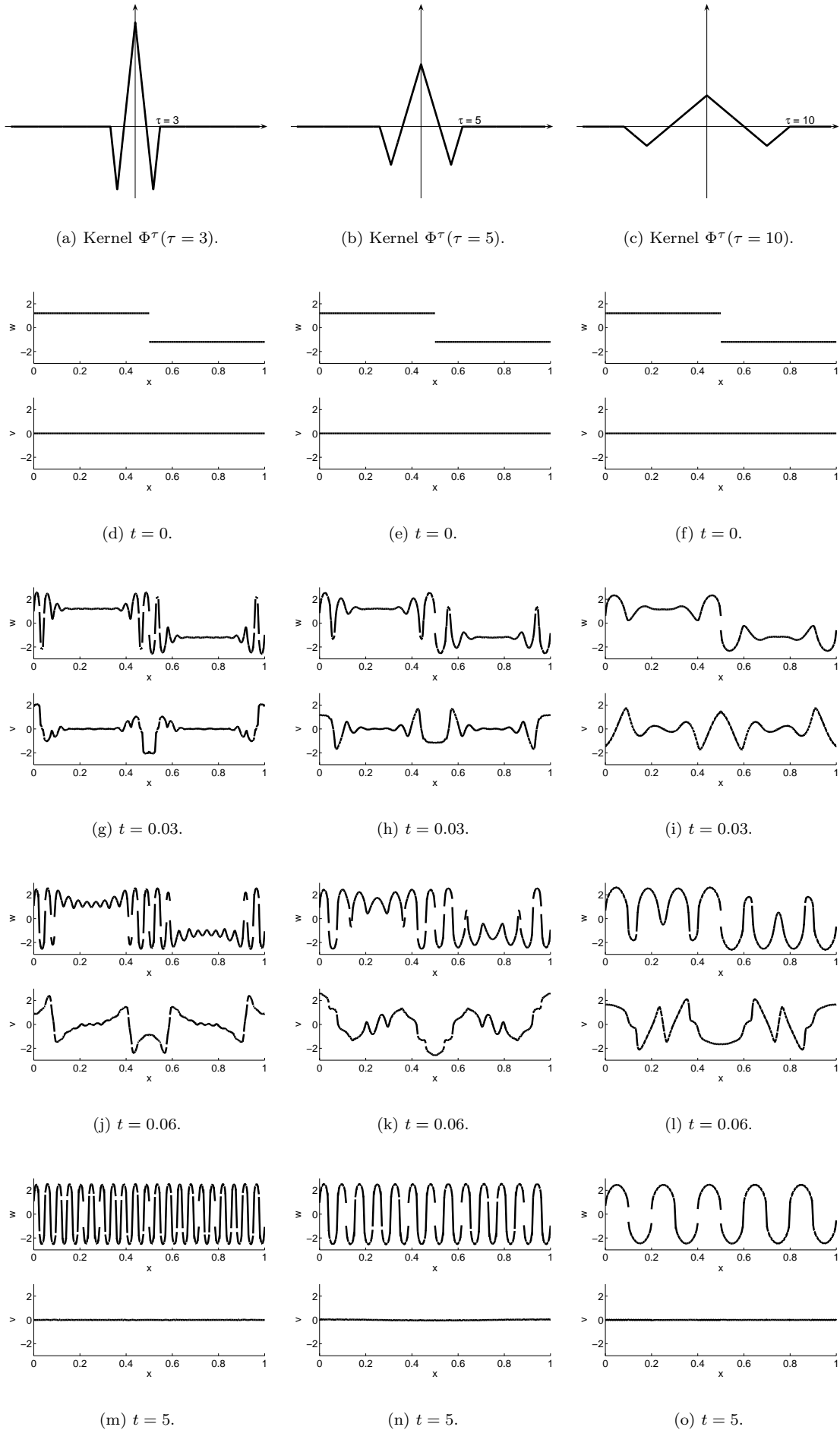


FIGURE 11. Numerical solutions for the non-local variant of (12) at different

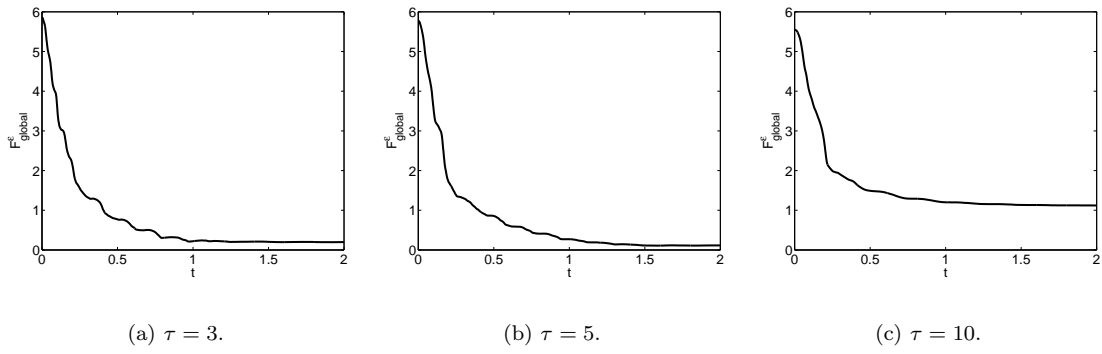


FIGURE 12. Energy behaviour for (12) with non-positive kernel functions  $\Phi^{\tau}$  as in (38).





## Erschienene Preprints ab Nummer 2007/001

Komplette Liste: <http://preprints.ians.uni-stuttgart.de>

- 2007/001 *Lehrstuhl Rohde, Lehrstuhl Wohlmuth, AG Sändig*: Jahresbericht IANS 2006
- 2007/002 *Dechevski, L.T., Wendland, W.L.*: On the Bramble-Hilbert Lemma, II
- 2007/003 *Hager, C., Wohlmuth, B.I.*: Analysis of a modified mass lumping method for the stabilization of frictional contact problems
- 2007/004 *Sändig, A.-M.*: Variational methods for nonlinear boundary value problems in elasticity. Lectures at the Charles University Prague, Feb.07
- 2007/005 *Dressel, A., Rohde, C.*: Global existence and uniqueness of solutions for a viscoelastic two-phase model with nonlocal capillarity
- 2007/006 *Dressel, A., Rohde, C.*: Time-asymptotic behaviour of weak solutions for a viscoelastic two-phase model with nonlocal capillarity
- 2007/007 *Kohr, M., Wendland, W.L.*: Boundary integral equations for a three-dimensional Brinkman flow problem
- 2007/008 *Sändig, A.-M.*: Vorlesung Mathematik für Informatiker und Softwaretechniker I, WS 2006/2007
- 2007/009 *Surulescu, C.*: On a Time-Dependent Fluid-Solid Coupling in 3D with Nonstandard Boundary Conditions
- 2007/010 *Melnyk, T.*: Homogenization of a Boundary-Value Problem with a Nonlinear Boundary Condition in a Thick Junction of Type 3:2:1
- 2007/011 *Haink, J., Rohde, C.*: Local Discontinuous-Galerkin Schemes for Model Problems in Phase Transition Theory